Microbial metabolism of food allergens determines the severity of IgE-mediated anaphylaxis

Elisa Sánchez-Martínez[1,x], Liam E. Rondeau[2,x], Manuel Garrido-Romero[1,3], Bruna Barbosa da Luz[2], Dominic A. Haas[2], Gavin Yuen[2], Peter Hall[2], Rebecca Dang[2], Xuan-Yu Wang[2], Lucía Moreno-Serna[1], Celia López-Sanz[1], Emilio Nuñez-Borque[1], Maria Garrido-Arandia[4], Araceli Diaz-Perales[4], Yolanda R. Carrasco[5], Joshua F.E. Koenig[6], Tina D. Walker[6], Manel Jordana[6], Elena F. Verdu[2], Michael G. Surette[2], Pedro Ojeda[7], Francisco Vega[8], Carlos Blanco[8], Wayne G. Shreffler[9], Sarita U. Patil[9], F. Javier Moreno[3], Rodrigo Jiménez-Saiz[1,6,10,y,*], Alberto Caminero[2,y,z,*]

[1]Department of Immunology, Instituto de Investigación Sanitaria Hospital Universitario de La Princesa (IIS-Princesa), Universidad Autónoma de Madrid (UAM), Madrid, Spain.

[2]Department of Medicine, Farncombe Family Digestive Health Research Institute, McMaster University, Hamilton, ON, Canada.

[3]Department of Bioactivity and Food Analysis, Instituto de Investigación en Ciencias de la Alimentación (CIAL), CSIC-UAM, CEI, Madrid, Spain.

[4]Centre for Plant Biotechnology and Genomics (CBGP), Universidad Politécnica de Madrid (UPM-INIA), Madrid, Spain.

[5]Department of Immunology and Oncology, Centro Nacional de Biotecnología (CNB)-CSIC, Madrid, Spain.

[6] Department of Medicine, McMaster Immunology Research Centre (MIRC), Schroeder Allergy and Immunology Research Institute (SAIRI), McMaster University, Hamilton, ON, Canada.

[7]Clínica de Asma y Alergia Dres. Ojeda, Madrid, Spain.

[8]Department of Allergy, Hospital Universitario de La Princesa, IIS-Princesa, Madrid, Spain.

[9]Food Allergy Center and Center for Immunology and Inflammatory Diseases, Massachusetts General Hospital, Boston, Massachusetts, USA.

[10]Faculty of Experimental Sciences, Universidad Francisco de Vitoria (UFV), Madrid, Spain.

[x]First co-authors who contributed equally to this work.
[y]Senior co-authors.
[z]Lead contact.
*Correspondence: rodrigo.jimenez@ufv.es / @R_JimenezSaiz (R.J.-S); acamine@mcmaster.ca (A.C.) / @LabCaminero

SUMMARY

Anaphylaxis is an acute, potentially life-threatening reaction, often triggered by foods and largely mediated by IgE. A critically important aspect of anaphylaxis pertains to the factors that modulate its severity. The human microbiota is known to influence oral tolerance, but the microbial mechanisms directly involved in IgE-mediated anaphylaxis remain unknown. Here, we demonstrate that human saliva harbors peanut-degrading bacteria that metabolize immunodominant allergens (Ara h 1 and Ara h 2) and alter IgE binding. Additionally, we provide *in vivo* evidence showing that oral bacteria metabolize peanut allergens, influencing systemic allergen exposure and the severity of anaphylaxis. Finally, in a clinical study, we observe that common peanut-degrading bacteria, such as *Rothia,* from the oral cavity, are more abundant in peanut-allergic patients who exhibit better tolerance to allergen exposure. Altogether, these results demonstrate the role of the human microbiota in modulating IgE-mediated reactions through allergen metabolism. These findings reveal a novel microbial mechanism with potential to prevent, or reduce, the severity of IgE-mediated anaphylaxis.

KEYWORDS

Allergens, Allergy, Anaphylaxis, IgE; Inflammation, Metabolism, Microbiota, Oral, Peanut, Saliva

INTRODUCTION

Inflammation typically serves to restore homeostasis in response to tissue damage or infection, yet it can cause immunopathology when exaggerated or inappropriate[1]. Anaphylaxis is a classic example of an immunopathological reaction that can lead to acute and potentially fatal outcomes within minutes. The main pathway of anaphylaxis is mediated by immunoglobulin (Ig)E and mast cells: upon allergen binding, mast cell-bound IgE induces their activation and the rapid release of inflammatory mediators like tryptase or histamine, which drive the acute clinical manifestations of anaphylaxis[2,3]. Foods are common anaphylaxis triggers, with peanut (PN) being the leading cause of food-induced anaphylaxis and allergy-related deaths among children[4,5]. This burden is aggravated by the persistence of PN-allergy in over 70% of individuals, the absence of curative treatments, and the high rate of accidental exposures despite patients' effort to avoid them[6-8].

An intricate aspect of anaphylaxis is understanding the factors that modulate the severity of food-induced allergic reactions. The severity of anaphylaxis is influenced by multiple factors, including genetic, environmental, dietary, and behavioural aspects, as well as co-factors and comorbidities[9,10]. However, despite these factors, clinical observations often reveal a disconnect between serum levels of allergen-specific IgE—the key molecule involved in food-induced anaphylaxis—and clinical reactivity[11-13]. Elucidating the factors that impact clinical reactivity is essential to better manage and reduce the risk of severe reactions in food-allergic individuals[3]. The human microbiota has gained considerable attention for its capacity to influence both oral tolerance and dietary antigen immunogenicity[14-17]. Indeed, studies have revealed differences in the intestinal microbiota composition of food-allergic patients[18-20]. Nonetheless, the microbial mechanisms involved in food-induced anaphylaxis remain largely unknown.

The oro-gastrointestinal microbiota is often regarded as a "second metabolic organ" capable of breaking down dietary components that are otherwise resistant to human digestive enzymes. Certain food allergens, including the immunodominant PN allergens Ara h 1 and Ara h 2[21,22], resist complete digestion by mammalian digestive enzymes[23,24]. In this study, we demonstrate that human saliva contains PN-degrading bacteria capable of metabolizing immunodominant allergens and modulating IgE-specific immunity. We also show the *in vivo* capacity of these bacteria to participate in PN-metabolism, thereby determining systemic allergen access and IgE-mediated anaphylaxis. Finally, in a clinical study, we describe that common PN-degrading bacteria, such as *Rothia* from the oral cavity, are more abundant in allergic patients who exhibit higher allergen threshold to controlled allergen exposure. These results demonstrate the human microbiota's ability to modulate IgE-mediated reactions through allergen metabolism and reveal a novel microbial mechanism with translational potential to prevent or mitigate IgE-mediated anaphylaxis.

RESULTS

Microbiota participates in peanut allergen metabolism

To study the role of microbes in PN metabolism, we used C57BL6 mice with and without microbiota (germ-free; GF). We selected mice with different microbiota compositions: specific pathogen-free (SPF) mice, which have a controlled and diverse microbiota, and altered Schaedler flora (ASF) mice, which harbor a stable microbiota with limited bacterial species (**Figure S1**). Mice were gavaged with crude PN protein extract (CPE) and sacrificed after 40 minutes (**Figure 1A**). The quantities of PN allergens Ara h 1 and Ara h 2 were higher in small intestinal content of GF mice and those with a limited ASF microbiota, compared to mice with a complex SPF microbiota (**Figure 1B**). We also detected variations in the concentrations of these allergens systemically. Compared to SPF mice, GF and ASF mice presented higher serum levels of Ara h 1 but lower serum levels of Ara h 2 (**Figure 1C**). To determine whether these differences were due to variations in the digestive capacity, intestinal contents of PN-naïve mice were incubated with CPE *ex vivo*. The intestinal contents of SPF mice degraded Ara h 1 and Ara h 2 more effectively than those of GF and ASF mice (**Figure 1D**). We hypothesized that microbial metabolism influenced the differences observed in PN allergen digestion and attempted to isolate PN-degrading bacteria from SPF and ASF mouse intestinal contents. Notably, PN-degrading bacteria were present in the small and large intestines of SPF mice but absent in ASF mice. While various PN-degrading bacterial species were identified, their capacity digest Ara h 1 and Ara h 2 varied by bacterial strain (**Figure 1E**). Together, these results demonstrate that the intestinal microbiota metabolizes PN allergens and influences their systemic availability.

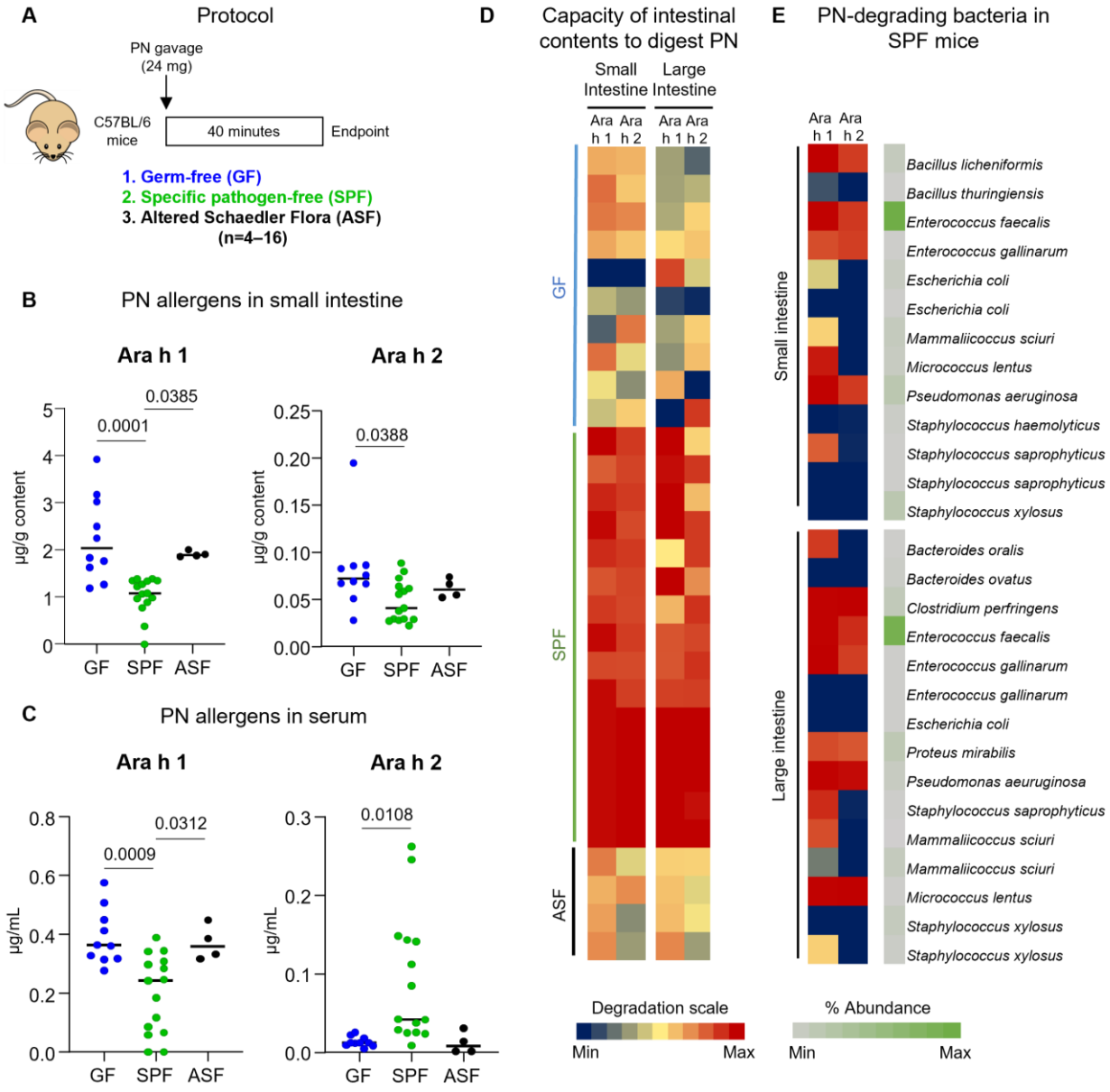

Figure 1. Microbiota participates in allergen metabolism *in vivo*.
(A) Experimental design. C57BL/6 mice with germ-free (GF), specific pathogen-free (SPF), and altered Schaedler flora (ASF) microbiota were provided a bolus of peanut (PN) intragastrically (i.g.). Peripheral blood and intestinal contents were collected 40 minutes post-PN delivery for analysis. n=4–16 mice per group. (B and C) PN allergens (Ara h 1 and Ara h 2) in small intestinal content (B) and serum from peripheral blood (C). Data are presented as mean where each dot represents an individual mouse. Displayed *P* values were calculated using one-way ANOVA with Tukey's post-hoc test. (D) Heatmap showing digestion capacity of GF, ASF, and SPF microbiota against Ara h 1 and Ara h 2. PN-naïve intestinal contents were incubated with PN allergens *in vitro* and remaining allergens were quantified after digestion. Each row represents one mouse. Statistical comparisons between groups were performed using a one-way ANOVA with Tukey's post-hoc test. Significance levels: Small intestine Ara h 1: GF vs. SPF ($P<0.0001$), ASF vs. SPF ($P=0.0290$). Small intestine Ara h 2: GF vs. SPF ($P<0.0001$), ASF vs. SPF ($P<0.0001$). Large intestine Ara h 1: GF vs. SPF ($P<0.0001$), ASF vs. SPF ($P=0.0289$). Large intestine Ara h 2: GF vs. SPF ($P<0.0001$), ASF vs. SPF ($P<0.0024$). (E) Heatmap showing digestion capacity and abundance of bacterial isolates from the small

and large intestine of SPF mice. Each row represents one bacterial isolate. Colour scales for (D) and (E): allergen degradation (blue-yellow-red) and % relative abundance (green). Refer also to Figure S1.

Mice lacking peanut-degrading bacteria exhibit severe anaphylaxis

To investigate the impact of microbial PN metabolism on acute allergic reactions, we used ASF and SPF C3H/HeN mice, a strain more susceptible to type 2 immunity and anaphylaxis upon oral PN challenge[25]. Consistent with our previous findings in C57BL/6 mice, ASF mice exhibited a reduced capacity to metabolize PN compared to SPF C3H/HeN mice (**Figure S2A–C**). ASF and SPF C3H/HeN mice were sensitized to PN with cholera toxin (CT) via intragastric (i.g.) administration once per week for 6 weeks, followed by an i.g. challenge with CPE to assess anaphylactic reactions to PN allergens (**Figure 2A**). ASF mice, which lack PN-degrading bacteria, had higher serum levels of PN-specific IgE than SPF mice (**Figure 2B**). They also exhibited higher serum levels of mucosal mast cell protease-1 (mMCP-1), indicating local activation of effector cells in the gastrointestinal tract, along with systemic hypothermia following PN challenge (**Figure 2C & Figure S3A**). To bypass the influence of microbial PN metabolism on IgE production, we sensitized SPF and ASF mice with PN + CT via intraperitoneal (i.p.) injection (**Figure 2A**). While both groups exhibited similar serum levels of PN-specific IgE (**Figure 2D**), ASF mice had higher serum mMCP-1 levels and developed hypothermia following PN challenge (**Figure 2E & Figure S3B)**. We further bypassed the endogenous capacity to generate allergen-specific IgE in the sensitization process by passively transferring serum from PN-allergic mice into SPF- and ASF-colonized mice (**Figure 2A; Figure S3D)**. Both mouse strains presented similar levels of PN-specific IgE in the serum after passive sensitization (**Figure 2F**). However, ASF mice again exhibited higher serum levels of mMCP-1 and hypothermia following PN challenge (**Figure 2G & Figure S3C**). These results demonstrate that the presence of certain microbes at the site of allergen challenge can protect from anaphylaxis.

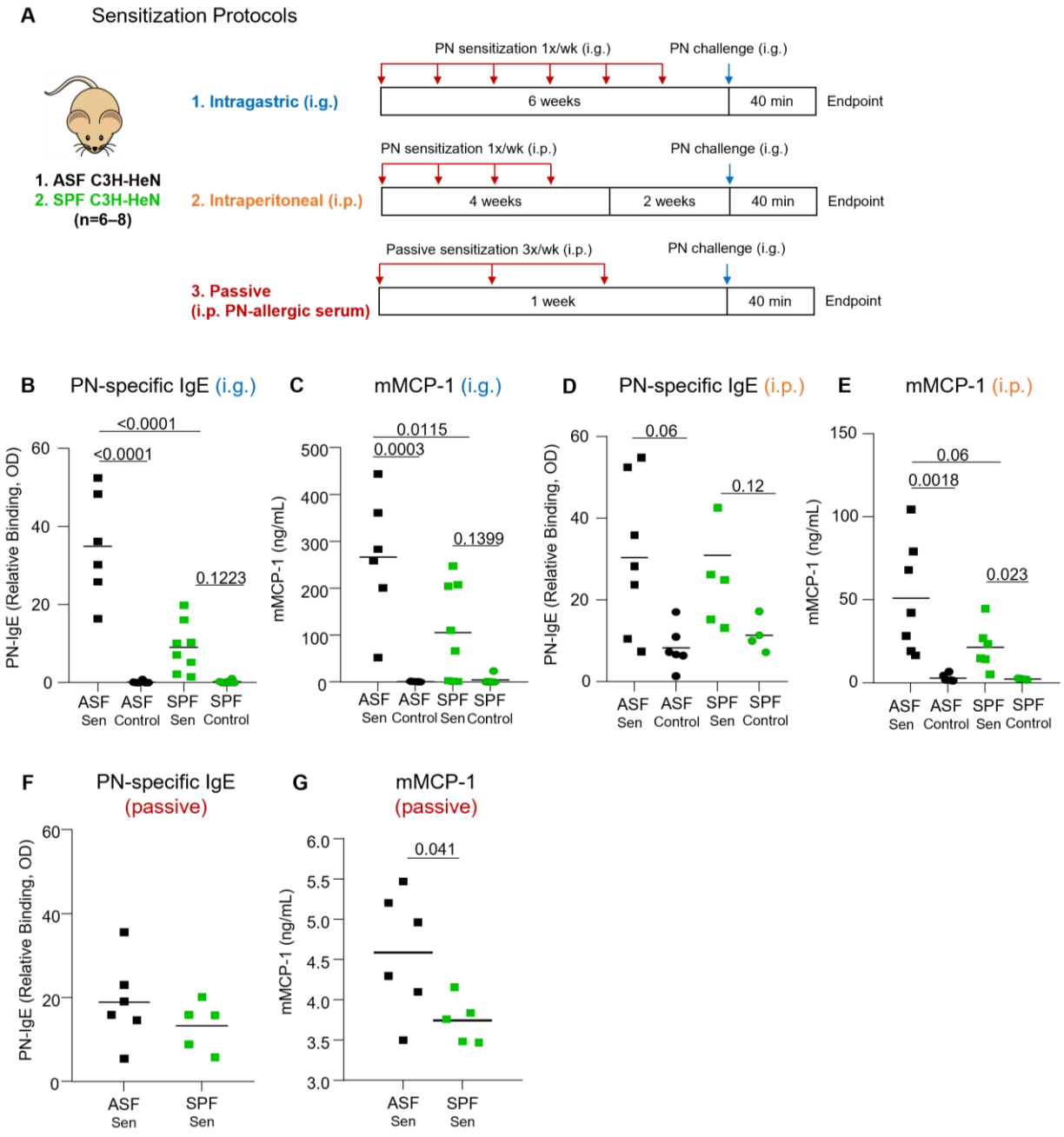

Figure 2. Mice lacking peanut-degrading bacteria present severe anaphylaxis.
(A) Experimental design for peanut (PN) sensitization and challenge of C3H-HeN mice colonized with specific pathogen-free (SPF) and altered Schaedler flora (ASF) microbiota. Mice were sensitized (1) intragastrically (i.g.; PN + cholera toxin) once per week for 6 weeks, (2) intraperitoneally (i.p.; PN + cholera toxin) once per week for 4 weeks, and (3) passively (i.p.; serum from PN-allergic mice) once every 48 hours, 3 times. Sensitized mice were challenged with a PN bolus i.g. after 7 weeks and sacrificed 40 minutes later. (B and C) Serum PN-specific IgE (B) and serum mucosal mast cell protease 1 (mMCP-1) (C) of i.g. sensitized ASF and SPF mice after PN challenge. (D and E) Serum PN-specific IgE (D) and serum mMCP-1 (E) of i.p. sensitized ASF and SPF mice after PN challenge. (F and G) Serum PN-specific IgE (F), serum mMCP-1 (G) passively sensitized ASF and SPF mice after PN challenge. Data are presented as mean where each dot represents an individual mouse. n=6-8 mice per group. Displayed *P* values were calculated

using one-way ANOVA with Tukey's post-hoc test (B and E) and Student's *t*-test (F and G). Refer also to Figures S2 and S3.

Human oral cavity harbors bacteria with the capacity to digest peanut

Food-induced acute allergic responses, including anaphylaxis, can occur within minutes of allergen exposure. Given this rapid onset, we investigated whether humans harbor PN-degrading bacteria in the oral cavity. Saliva samples were collected from 13 volunteers with no reported food allergies **(Table S1)**. Analysis of the oral microbiota composition via 16S rRNA sequencing revealed donor-specific profiles, with *Prevotella*, *Rothia,* and *Fusobacterium* as the most abundant genera (**Figure 3A**). We then plated saliva samples on PN-enriched media agar to isolate bacteria with PN-degrading capacity, selecting strains that produced a hydrolytic halo, indicating their ability to degrade PN (**Figure 3B**). PN-degrading bacteria were detected in nearly all donors, with *Rothia, Staphylococcus, Streptococcus,* and *Veillonella* being the most frequently isolated genera. Each isolated bacterial strain was then incubated with CPE to facilitate allergen digestion, and the remaining Ara h 1 and Ara h 2 were quantified using specific antibodies. Additionally, we screened a well-characterized bacterial collection for PN-degrading potential[26]. While many bacterial strains exhibited PN digestion capabilities on agar plates, their capacity to degrade the main allergens varied by taxon and strain (**Figure 3C**). *Rothia*, a dominant genus in the oral cavity (10-40% relative abundance), consistently degraded Ara h 1 and Ara h 2 *in vitro*. This activity was observed in all tested *Rothia* strains and a phylogenetically related genus, *Micrococcus*, suggesting a conserved PN-degrading function (**Figure 3C**). In contrast, most strains from other PN-degrading genera such as *Gemella* or *Streptococcus* lacked significant allergen-degrading capacity (**Figure S4A**). While *Staphylococcus* strains showed strong PN-degrading potential, their ability to break down key PN allergens was strain-specific (**Figure 3C**). Altogether, these findings demonstrate the presence of PN-degrading bacteria in the oral cavity, each exhibiting varying capacities to degrade immunodominant PN allergens.

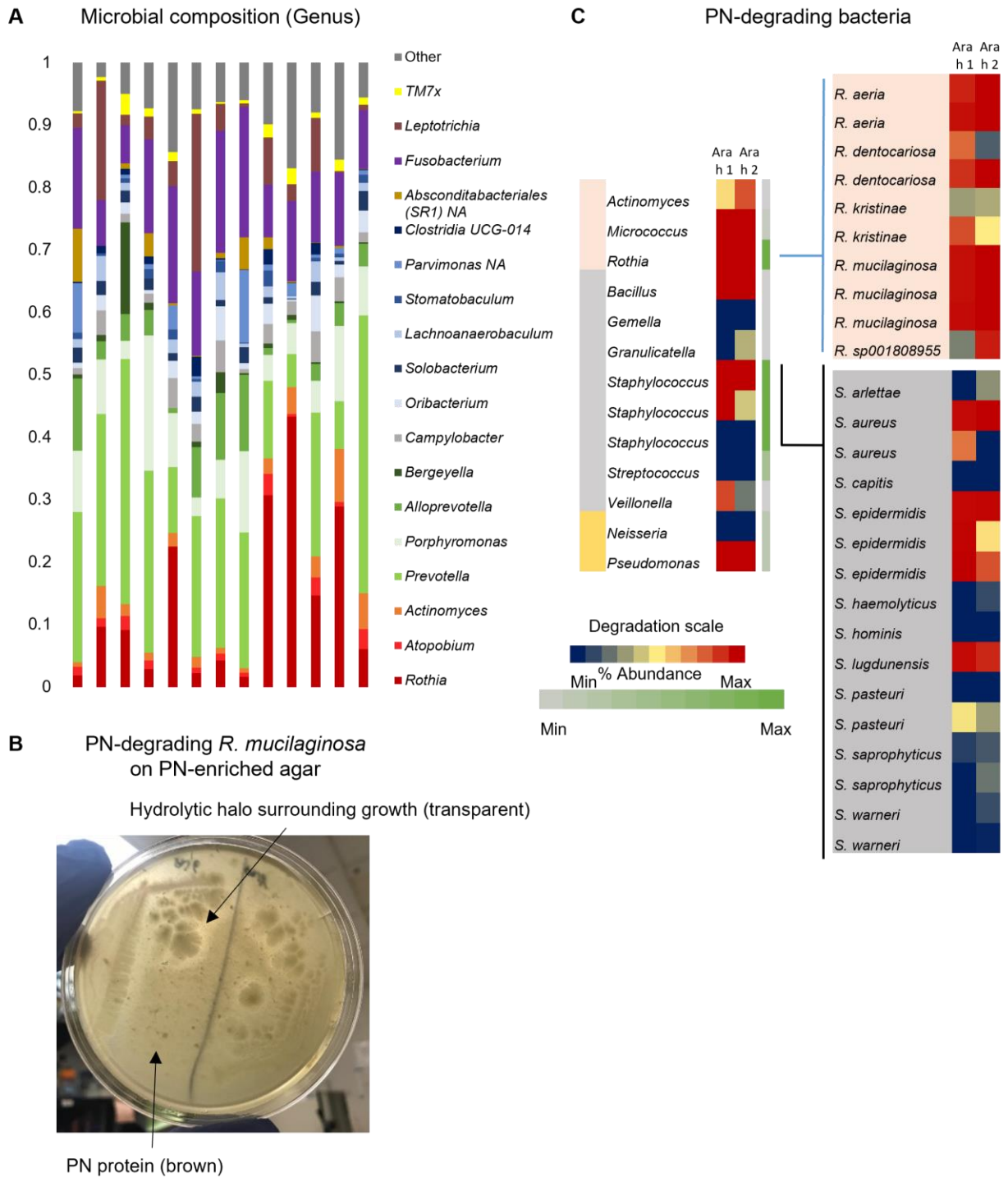

Figure 3. Human saliva harbors peanut-degrading bacteria.
(A) Genus-level relative abundance of the microbial composition of saliva samples collected from individuals without peanut (PN) allergy. Each bar represents one individual (n=13). Taxa lower than 0.01 relative abundance are not shown. (B) Representative image of PN-degrading bacteria (*Rothia mucilaginosa*) isolated from human saliva on PN-enriched agar. Zone of clearance of PN surrounding bacterial growth indicates PN degradation. (C) Identification of PN-degrading bacteria isolated from human saliva. Bacteria shown were identified for whole PN-degradation by growth on PN-enriched agar and further characterized by their capacity to degrade Ara h 1 and Ara h 2. Heatmaps show the capacity to degrade

Ara h 1 and Ara h 2 (blue-yellow-red scale), and abundance of isolated bacteria (% of relative abundance based on total number of isolated strains; green scale). Data are presented at the genus and species levels for Actinomycetota (pink), Bacillota (grey) and Pseudomonota (Yellow). Refer also to Figure S4.

Peanut allergens are degraded by bacteria

To further study the microbial capacity for PN allergen digestion, we conducted proteomic analyses focusing on key bacterial taxa. We selected two primary genera: *Rothia*, a dominant oral taxon with efficient allergen-digestion capacity, and *Staphylococcus,* which has been previously associated with allergic diseases (**Figure S4B**)[27]. First, we confirmed the capacity of these taxa to degrade the main PN allergens Ara h 1 (64 kDa) and Ara h 2 (17 kDa) using SDS-PAGE (**Figure 4A–B**). To strengthen these data, we performed tandem mass spectrometry analysis on the fraction below 3 kDa, screening for PN-derived peptides after bacterial digestion. Given the low relative abundance of Ara h 2 in the PN matrix (5.9-9.3% of total protein) and the noise introduced by bacterial proteins in the samples, we centered the proteomic analyses on Ara h 1 (12-16% of total protein)[28]. We identified several Ara h 1-derived peptides following PN digestion by strains of *Rothia* and *Staphylococcus*. As expected, we quantified more peptides from bacterial strains that degraded PN more extensively (*Rothia* R3, 6 peptides; S1, 9 peptides), according to the electrophoretic analysis. Using molecular modelling, we visualized these peptides, marking in yellow peptides digested by bacteria (**Figure 4C–F**). Interestingly, some of the identified peptides, shown in purple, have been reported as clinically relevant IgE epitopes recognized by PN-allergic patients[29-31]. These epitopes are distributed across various regions of the 3D structure of Ara h 1, highlighting the lack of localization of the identified peptides to a single structural domain (**Figure 4C–F**). Considering the ability of these *Rothia* and *Staphylococcus* species to degrade PN, we evaluated their impact on human IgE binding to PN after bacterial digestion by Western blotting. We used a pool of sera from PN-allergic patients with elevated levels of Ara h 1- and Ara h 2-specific IgE (**Table S2**). The analysis showed a substantial reduction in IgE-binding to PN proteins overall, and to Ara h 1 and Ara h 2 in particular (**Figure 4G–H**). To precisely define the impact of microbial metabolism on main PN allergens, we mono-sensitized mice to native Ara h 1 or recombinant Ara h 2 and used their sera to analyze IgE recognition of the digested PN fragments via Western blotting (**Figure 4I–J**). *Rothia* digestion of PN reduced IgE binding to Ara h 1, most notably by strain R3. Similarly, *Staphylococcus* strains (S1 and S3) completely degraded and reduced IgE-binding to Ara h 1, though some residual fragments retained IgE binding capacity. *Staphylococcus* strains with lower PN-degrading capacity, such as S2, showed less efficacy in reducing binding to Ara h 1 (**Figure 4I)**. On the other hand, sera from mice sensitized with recombinant Ara h 2 predominantly recognized a band around ~37 kDa, likely representing its oligomerized forms. Nevertheless, PN-digestion by *Rothia* strains impaired Ara h 2 recognition by IgE, particularly with strain R3. *Staphylococcus* strains S1 and S3 also reduced IgE-binding to Ara h 2, while strain S2 showed little effect (**Figure 4J)**. Altogether, these findings demonstrate the potential of *Rothia* and *Staphylococcus* strains to modify the structure of

key PN allergens, including IgE-binding epitopes, and thereby altering their recognition by both murine and human IgE.

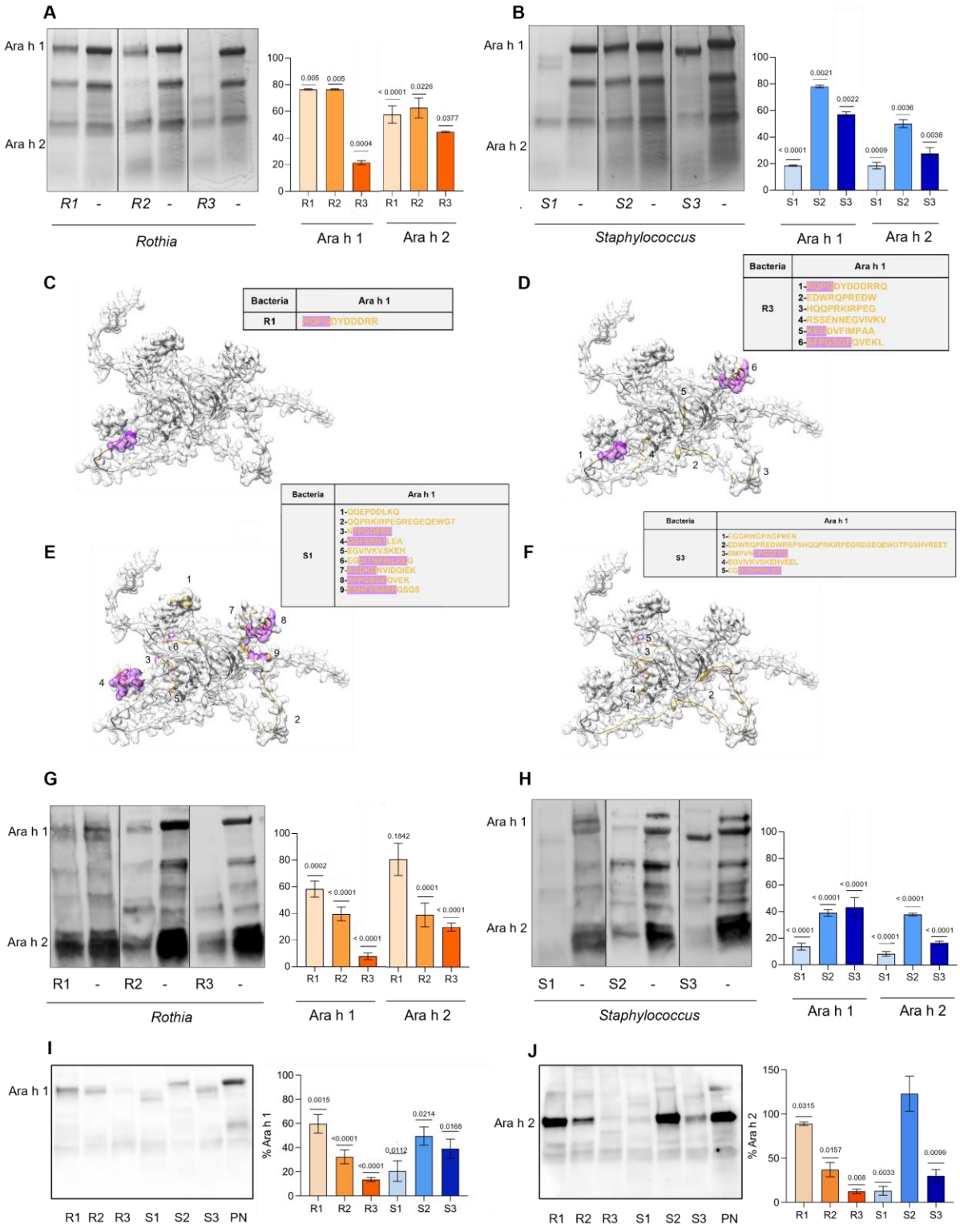

Figure 4. Peanut allergens are degraded by *Rothia* and *Staphylococcus*. Selected *Rothia* (R1- *Rothia aeria,* R2- *Rothia dentacariosa,* and R3- *Rothia mucilaginosa*) and *Staphylococcus* (S1- *Staphylococcus epidermidis,* S2- *Staphylococcus aureus*, and S3- *Staphylococcus aureus*) strains were incubated with crude peanut (PN) protein extract (CPE) in liquid media before characterization of PN allergen (Ara h 1 and Ara h 2) degradation. (A and B) SDS-PAGE analysis of Ara h 1 (64 kDa) and Ara h 2 (17 kDa) degradation by *Rothia* (A) and *Staphylococcus* (B). (C to F) Molecular modeling of Ara h 1 (Alphafold database code: AF-P43238-F1), in yellow are marked the peptides below 3 kDa identified by mass spectrometry following digestion by R1 (C), R3 (D), S1 (E), and S3 (F); in purple are marked the immunopeptides recognized by human IgE. (G and H) Western blot showing binding of PN-allergic human IgE to PN allergens after *Rothia* (G) and *Staphylococcus* (H) digestion. (I) Western blot showing IgE from Ara h 1-sensitized mice binding to Ara h 1 after bacterial digestion. (J) Western blot showing IgE from Ara h 2-sensitized mice binding to Ara h 2 after bacterial digestion. Bar charts indicate quantification of allergens remaining after bacterial digestion. Data are presented as the mean ± SEM of each group. Displayed *P* values were calculated using an unpaired *t*-test between undigested PN and bacterially digested PN in every panel of the figure.

Microbial metabolism mitigates peanut allergenicity

The structural modifications of Ara h 1 and Ara h 2 caused by microbial metabolism affected IgE recognition, prompting us to assess the functional consequences using a mast cell activation assay[32,33]. We sensitized bone marrow-derived mast cells (BMMCs) with sera from mice allergic to either native Ara h 1 or recombinant Ara h 2 and assessed IgE-mediated mast cell activation after challenge with bacterial PN digests. This was done by challenging the BMMCs with either PN-bacterial digests or undigested PN, and measuring CD63 and CD107a surface expression, along with β-hexosaminidase activity in the cell supernatants (**Figure 5 & Figure S5A**). Our initial controls confirmed that serum from Ara h 1-allergic mice induced BMMC activation following Ara h 1 or CPE challenge, but not upon Ara h 2 stimulation, and vice versa (**Figure S5B–C**). We then observed that, among the three *Rothia* strains, PN-digestion by strain R2 consistently reduced BMMC activation for both Ara h 1 and Ara h 2 (**Figure 5A–B**); while PN-digestion by strains R1 and R3 significantly decreased BMMC responses in Ara h 2-sensitized cells (**Figure 5A–B**). On the other hand, among the three *Staphylococcus* strains, PN-digestion by strain S1 significantly reduced BMMC activation in Ara h 1-sensitized cells **(Figure 5C)**, while BMMC responses to Ara h 2 were impaired by the digestion of the three strains (**Figure 5D**). In sum, these results demonstrate that the metabolism of key PN allergens by human oral bacteria can modulate the ability of these allergens to trigger IgE-mediated mast cell activation.

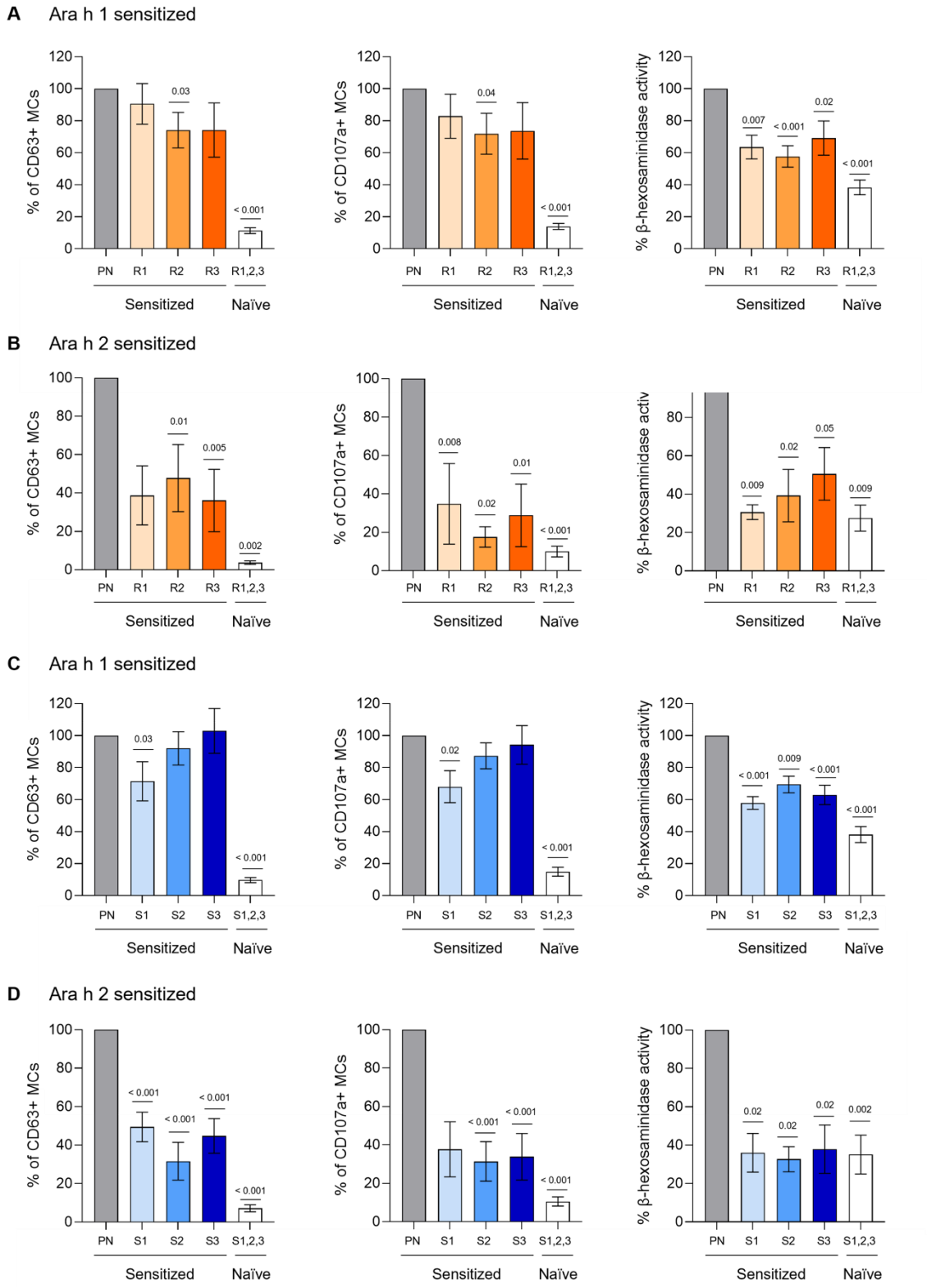

Figure 5. Challenge with bacterially digested peanut impairs mast cell activation. Mast cells (MCs) were sensitized with pooled sera from mice allergic to Ara h 1 or Ara h 2 and then challenged with undigested peanut (PN; gray) as a positive control or with PN digested by bacteria (orange for *Rothia*, blue

for *Staphylococcus*). The bacterial strains used were R1—*Rothia aeria*, R2—*Rothia dentocariosa*, R3—*Rothia mucilaginosa* (A, B) and S1—*Staphylococcus epidermidis*, S2—*Staphylococcus aureus*, S3—*Staphylococcus aureus* (C, D). Negative controls (white bars) consisted of MCs sensitized with sera from non-allergic mice and challenged with PN digested by bacteria. The bar graphs indicate CD63 or CD107a expression and β-hexosaminidase activity, normalized to 100% to allow data comparison across different experiments. Data are presented as mean ± SEM for each group. While all three *Rothia* and *Staphylococcus* strains are displayed in the same graphs, statistical analyses were performed separately for each bacterium against its respective control. P-values were calculated using one-way ANOVA with Dunnett's post-hoc test when comparing against undigested PN in all panels, except for R1-CD63-Ara h 2 (B), S2-CD107a-Ara h 1 (C), and S1-CD107a-Ara h 2 (D), where the Kruskal-Wallis test with Dunn's post-hoc correction was used instead. The negative control includes pooled results from naïve MCs challenged with PN digested by all three *Rothia* and *Staphylococcus* species. Statistical comparisons against undigested PN were conducted using one-way ANOVA with Dunnett's post-hoc test for β-hexosaminidase activity (D), CD63 (A), and CD107a (A-C), or the Kruskal-Wallis test with Dunn's post-hoc correction for β-hexosaminidase activity (A-C), CD63 (B-D), and CD107a (D). Refer also to Figure S5.

Microbial peanut metabolism alters systemic allergen access

To study the *in vivo* capacity of human oral bacteria to degrade PN allergens, we colonized GF C57BL/6 mice with bacterial strains exhibiting varying allergen-degrading capacities. We selected three *Staphylococcus* strains based on their PN-degrading capacity *in vitro*: one with strong capacity to degrade both Ara h 1 and Ara h 2 (S1), one that degrades only Ara h 1 (S3), and one with no detectable allergen-degrading capacity (S2). Additionally, we included a *Rothia* strain (R3) capable of degrading both Ara h 1 and Ara h 2. GF mice were used as controls. After colonization, mice were gavaged with CPE (**Figure 6A**), as previously described for SPF and ASF mice. Successful transfer of PN-degrading capacity was confirmed in colonized mice (**Figure 6B**). Notably, we observed a reduction in Ara h 1 and Ara h 2 levels in the small intestinal content of mice colonized with allergen-degrading bacteria, such as S1 and R3 (**Figure 6C**). Additionally, systemic levels of Ara h 1 and Ara h 2 were reduced in these mice **(Figure 6D)**. In contrast, Ara h 1—and particularly Ara h 2—showed increased systemic levels in mice colonized with PN-degrading bacteria that had impaired allergen-degrading capacity (S2) (**Figure 6D**). To study whether bacterial metabolism alters allergen passage through the mucosa and subsequent systemic access, we assessed allergen translocation across *ex vivo* mouse small intestinal tissue using Ussing chambers. CPE, pre-incubated with or without the different bacterial strains was applied to the mucosal side of the chamber, and Ara h 1 and Ara h 2 levels were quantified on the serosal side of the tissue after 2 hours. We found that PN-degrading bacteria with impaired allergen-degrading capacity facilitated the passage of Ara h 1 and Ara h 2 through the intestinal mucosa (**Figure 6E**). These findings suggest that bacteria metabolize PN *in vivo* and control allergen passage through the intestinal mucosal barrier.

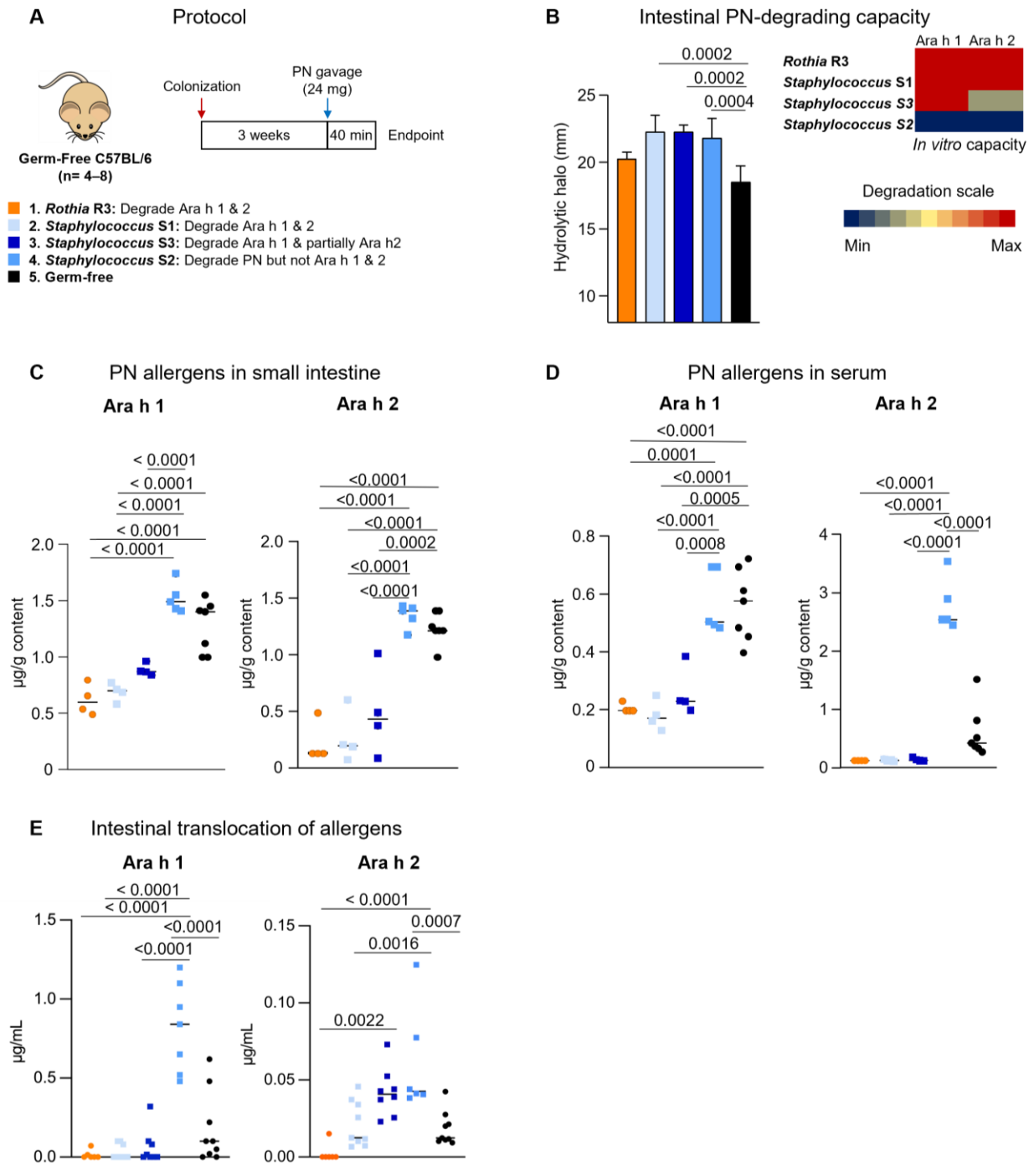

Figure 6. Bacteria dictate systemic access of allergens *in vivo*.
(A) Experimental design. Germ-free C57BL/6 mice were mono-colonized with bacteria (R3– *Rothia mucilaginosa*, S1- *Staphylococcus epidermidis* S2- *Staphylococcus aureus*, and S3- *Staphylococcus aureus*) with different capacities to digest peanut (PN) allergens. One group of mice maintained germ-free served as controls. Mice were provided a PN bolus intra-gastrically 3 weeks after colonization and sacrificed 40 min later. (B) PN-degrading capacity of small intestinal content of mice mono-colonized with different bacteria and germ-free control as determined the diameter of PN hydrolytic halo, and degradation of Ara h 1 and Ara h 2. (C and D) PN allergens, Ara h 1 and Ara h 2 in small intestinal content (C) and serum from

peripheral blood (D). (E) Translocation of PN allergens digested by bacteria (R3 (orange), S1 (light blue), S3 (dark blue), S2 (medium blue), or non-growth control (black)) from the mucosal to serosal side of small intestinal tissue in Ussing chambers. Data are presented as mean + SD (B) and mean where each dot represents an individual mouse (C, D, E). n=4–8 mice per group. Displayed *P* values were calculated using a one-way ANOVA with Tukey's post-hoc test.

Microbial peanut metabolism dictates anaphylactic reactions *in vivo*

To evaluate the impact of microbial PN metabolism on anaphylactic responses, ASF C3H/HeN mice—which have impaired microbial PN metabolism and are susceptible to anaphylactic reactions upon oral exposure—were sensitized to PN via i.p. injection and subsequently challenged with bacterially pre-digested PN (**Figure 7A**). Four groups of mice received an i.g. PN challenge with either untreated PN (control) or PN pre-digested by one of the following bacteria: a) *Rothia* R1, b) *Staphylococcus* S1, or c) *Staphylococcus* S2, each exhibiting distinct allergen-degrading capacities. While all groups showed similar PN-specific IgE levels after sensitization (**Figure 7B**), serum mMCP-1 levels were lower in mice challenged with microbially pre-digested PN (**Figure 7C**). Notably, mice challenged with PN pre-digested by *Staphylococcus* S2, which has limited allergen-reducing capacity, exhibited higher serum levels mMCP-1. In a subsequent experiment, additional ASF C3H/HeN mice were sensitized to PN (i.p.) and then colonized with *Rothia* strains with efficient PN-degrading capacity (**Figure 7D**). After sensitization, ASF mice with and without PN-degrading bacteria were challenged to PN i.g. Despite having similar PN-specific IgE levels in serum after sensitization (**Figure 7E**), mice colonized with *Rothia* strains capable of digesting PN allergens demonstrated significantly reduced serum mMCP-1 levels (**Figure 7F**). Overall, these findings highlight the critical role of microbial allergen metabolism in modulating allergic responses *in vivo*.

Peanut-degrading bacteria are increased in allergic patients better tolerating peanut

To investigate the role of the oral microbiota in allergic reactions, we collected saliva samples from a small well-defined cohort of PN-allergic patients (**Figure 7G & Table S1)**. Prior to initiating oral immunotherapy (OIT), allergic patients underwent PN challenge to determine their threshold for reactivity (PN threshold), guiding OIT practices. We analyzed serum levels of IgE and the composition of the oral microbiota. Notably, serum levels of IgE specific to Ara h 1 and Ara h 2 showed a poor association with PN threshold **(Figure 7H)**, suggesting the role of additional factors. Examining the oral microbiota, we observed non-significant clustering based on PN threshold (**Figure S6)**. While PN-degrading taxa were present across patients with varying PN thresholds, individuals with higher PN thresholds exhibited a greater abundance of taxa capable of degrading Ara h 2 **(Figure 7I)**. Notably, *Micrococcales*—a taxon that includes *Rothia* and *Micrococcus*, both efficient at degrading immunodominant Ara h 1 and Ara h 2—was reduced in highly sensitive allergic patients with low PN threshold (0–40 mg), independent of serum Ara h

2-specific IgE levels (**Figure 7J**). Conversely, patients with high levels of Ara h 2-specific IgE with higher PN threshold showed an increased relative abundance of *Micrococcales*. These findings suggest that the oral microbiota could serve as a predictive marker of threshold reactivity to PN, highlighting the potential importance of microbial allergen metabolism in IgE-mediated reactions.

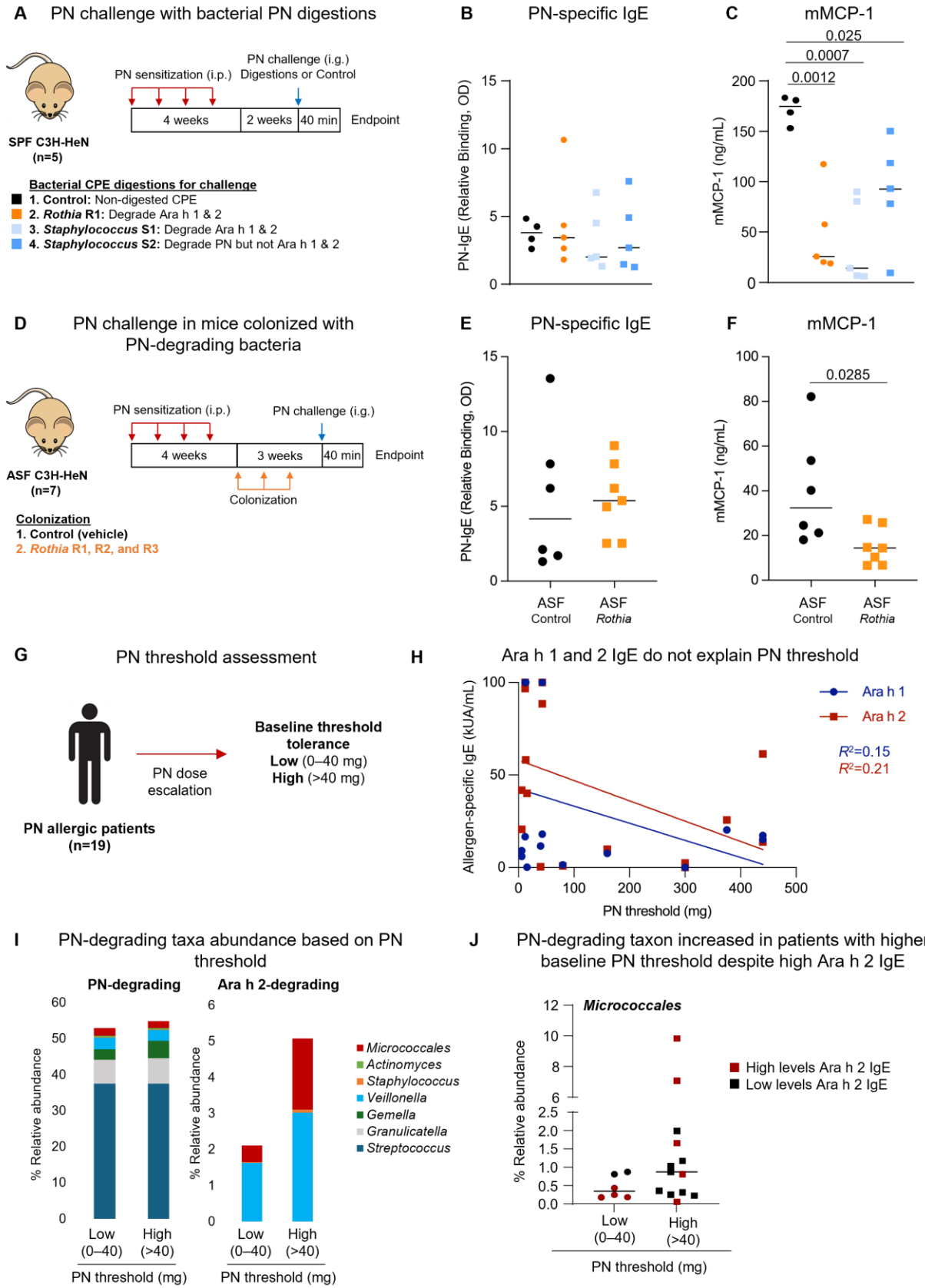

Figure 7. Microbial peanut metabolism reduces allergic reactions *in vivo* and is associated with allergen tolerance.
(A) Experimental design. Specific pathogen-free (SPF) C3H-HeN mice were sensitized intra-peritoneally (i.p.) to peanut (PN) once per week for 4 weeks. Sensitized mice were challenged intra-gastrically (i.g.) after 7 weeks with a bolus of PN previously digested by *Rothia* (R3), *Staphylococcus epidermidis* (S1), and *Staphylococcus aureus* (S2), or a non-digested control containing 24 mg of PN. Mice were sacrificed 40 minutes later. Heatmap represents the capacity of bacteria to degrade PN allergens *in vitro*. n=5 mice per group. (B) Serum PN-specific IgE before PN challenge. (C) Serum mucosal mast cell protease 1 (mMCP-1) after PN challenge. (D) Experimental design. C3H-HeN mice with altered Schaedler flora (ASF) microbiota sensitized i.p. to PN once per week for 4 weeks. One week after the last sensitization, mice were co-colonized with *Rothia* strains once per week for three weeks. Mice were provided a PN bolus i.g. three weeks after the first colonization and sacrificed 40 minutes later. n=7 mice per group. (E) Serum PN-specific IgE before PN challenge. (F) Serum mMCP-1 after PN challenge. (G) Experimental design. PN-allergic patients (n=19) were tested for PN threshold (low – 0-40 mg PN; high - >40 mg PN) using increasing PN concentrations before enrolment in oral immunotherapy (OIT). (H) Correlation plot of Ara h 1-specific IgE (y= -0.09x + 42.45, R^2 = 0.15, P=0.11) and Ara h 2-specific IgE (y= -0.11x + 58, R^2= 0.21, P=0.06) against PN threshold. (I) Relative abundance (%) of PN-degrading and Ara h 2-degrading bacteria in patients with low (0-40 mg) and high (>40 mg) PN threshold. (J) Relative abundance of *Micrococalles* in patients with low (0-40 mg) and high (>40 mg) PN threshold. Dot colour represents high (≥20 kUA/mL, red) and low (<20 kUA/mL, black) Ara h 2 IgE in serum. Data are presented as mean where each dot represents an individual mouse. Displayed P values were calculated using a one-way ANOVA with Tukey's post-hoc test (C, D) and unpaired Student's t-test (F, G). Refer also to Figure S6.

DISCUSSION

The human microbiome is essential for maintaining homeostasis, and disruptions in its composition are associated with immune disorders. The oro-gastrointestinal microbiota has gained attention for its role in influencing oral tolerance and sensitization to food antigens[14-16,34]. While studies have reported differences in the intestinal microbiota composition of food-allergic patients[18-20], the microbial mechanisms underlying food-induced anaphylaxis remain largely unknown. In this study, we show that human saliva harbors allergen-degrading bacteria capable of metabolizing immunodominant PN allergens, thereby modulating IgE-mediated reactions to foods. Identifying the microbes involved in PN metabolism in humans and characterizing the related microbially-mediated IgE-specific immune responses could have implications for reducing the severity of allergic reactions.

The antigenic properties of many foods are attributed to their resistance to gastrointestinal digestion[23,24]. Dietary allergens, such as those from PN, are poorly metabolized by human digestive enzymes[21,22]. However, the intestinal microbiota possesses a vast repertoire of metabolic pathways absent in humans, that participate in food digestion[35]. For example, the capacity of the intestinal microbiota to degrade other recalcitrant antigenic proteins, such as gluten[36], has been demonstrated[37,38]. Here, using gnotobiotic mouse models, we demonstrate that the microbiota contributes to PN allergen metabolism *in vivo*, with its composition influencing the amount of allergen reaching the intestine and circulation. While the intestinal microbiota affects host metabolism and food-dependent immune responses through mechanisms such as altering the intestinal barrier, motility, or immune

activation[14,39-41], we confirmed the presence of PN-degrading bacteria capable of digesting Ara h 1 and Ara h 2 along the gastrointestinal tract in wild-type SPF mice. These findings reveal the role of the intestinal microbiota in allergen metabolism and raise important questions about the impact of diet-microbiota interactions on food allergies.

Food allergies are mostly mediated by IgE[42], which, unlike other antibodies, can trigger life-threatening reactions to minute amounts of allergen[2]. We hypothesized that microbial metabolism could modulate IgE-mediated reactions to PN. First, we demonstrated that mice with defective PN-degrading capacity (ASF mice) developed more severe allergic reactions to PN than those with efficient PN metabolism (wild-type SPF mice) following i.g. sensitization and challenge. ASF mice also exhibited greater mucosal mast cell activation, likely increasing intestinal permeability and facilitating systemic allergen access[43,44]—a critical step in IgE-mediated anaphylaxis[45]. Intriguingly, ASF mice also developed higher titers of antigen-specific IgE than SPF controls, potentially due to their reduced ability to metabolize PN allergens. Similar increases in antigen-specific IgE have been reported in GF mice and mice colonized with limited microbial communities following sensitization[46-48]. Given that food-induced anaphylaxis is largely IgE-dependent[49,50], and that the microbiota may influence IgE-mediated food sensitization independently of allergen degradation[14], differences in sensitization between mouse strains could explain the severity of allergic reactions. To bypass local microbial factors, we evaluated the role of microbial metabolism in IgE-mediated food responses using additional models of systemic[51] and passive[33,52] sensitization. Following PN challenge, ASF mice with defective PN-degrading capacity developed more severe allergic reactions, characterized by increased mast cell degranulation and hypothermia, compared to conventional mice, despite similar PN-IgE titers. Altogether, these results indicate that microbial metabolism plays a crucial role in shaping IgE-mediated allergic reactions to foods in mice.

Food-induced anaphylaxis is usually caused by accidental allergen exposure through food consumption, posing a persistent threat that significantly impacts the quality of life of patients and their families[53,54]. Although several co-factors—such as exercise, estrogen levels, alcohol, and drugs—have been associated with an increased risk of anaphylaxis[10,55], the variations in allergen thresholds and individual susceptibility to anaphylaxis remain poorly understood. A recent study of subjects with accidental food-induced allergic reactions demonstrated that anaphylaxis severity is independent of the amount of allergen ingested, emphasizing individual sensitivity and the potential role of microbiota in modulating systemic access of PN[56]. To explore the potential role of microbial allergen metabolism in humans, we first searched for PN-degrading bacteria in healthy donors. We focused on the oral cavity, where ingested food first interacts with the oral microbiota, as anaphylactic reactions typically occur shortly after allergen exposure. While most microbiota research has centered on the large intestinal lumen due to its ease of sampling and high bacterial density, recent studies have highlighted the stability and complexity of the oral microbiota, as well as its relevance in health and disease[57]. Moreover, the oral microbiota serves as a continuous source of bacteria for the intestinal tract, seeding the small intestine with taxa such as *Rothia* and *Staphylococcus*[58], where

they may persist and contribute to allergen metabolism as food moves through the upper gastrointestinal tract[59]. Given this microbial continuity, studying intestinal colonization provides a complementary perspective on the functional contributions of these bacteria beyond their initial presence in the oral cavity, particularly in contexts where they influence allergen processing throughout the gut. Using techniques including SDS-PAGE, Western blotting, and proteomics, we confirmed the presence of PN-degrading bacteria in the oral cavity, which displayed varying capacities to degrade immunodominant PN allergens. Notably, different members of the oral microbiota disrupted epitopes critical for human IgE recognition and altered IgE binding of sera from PN-allergic patients and mice sensitized to Ara h 1 or 2. Overall, these results confirm the capacity of bacteria to potentially alter allergenicity in the oral cavity of humans.

Dominant taxa in the oral cavity such as *Rothia*, and phylogenetically related taxa, such as *Micrococcus*, demonstrated a consistent capacity to digest both Ara h 1 and Ara h 2 *in vitro,* thereby altering IgE recognition. The capacity of *Rothia* to degrade other dietary antigens such as gluten proteins has been also suggested[60,61]. Remarkably, impaired IgE recognition of PN upon *Rothia* digestion hampered the activation of the classical pathway of anaphylaxis both *in vitro* (mast cell assays) and *in vivo* (PN-allergic mice challenged with digested PN). In addition, the PN-degrading capacity of *Rothia* was validated *in vivo*, reducing the concentration of major PN allergens reaching the small intestine and circulation. We also tested the capacity of *Rothia* strains to alter IgE-mediated reactions following colonization in a competitive environment. To avoid changes in the adaptive immune response, ASF mice were colonized following sensitization. ASF mice colonized with *Rothia* ameliorated IgE-mediated reactions and mucosal mast cell activation upon challenge, in comparison to ASF controls. These data demonstrate that bacteria with PN-degrading capacity can modulate acute allergic responses *in vivo*.

Microbial PN metabolism does not always confer protection against IgE-mediated responses. Certain PN-degrading genera, such as *Gemella* or *Streptococcus,* lacked allergen-degrading capacity *in vitro*. However, *Staphylococcus,* a main PN-degrading taxon in the oral cavity*,* displayed strain-specific effects in our work. Others have reported that skin colonization by *Staphylococcus aureus* induces keratinocyte release of IL-36α[62], a pro-inflammatory cytokine linked to allergic sensitization to foods[27]. Additionally, *Staphylococcus* and other microbial proteases can induce immune activation and low-grade inflammation in the colon[63], and promote inflammatory responses to innocuous antigens[64,65]. Our findings revealed that *Staphylococcus* strains vary in their capacity to remove PN allergens and alter IgE-mediated recognition and mast cell activation *in vitro*. In gnotobiotic mice colonized with *Staphylococcus* strains exhibiting differing PN-degrading capacities, efficient strains reduced Ara h 1 and Ara h 2 levels in the small intestine and serum. However, these immunodominant peptides increased systemically in mice colonized with a strain lacking efficient PN-degrading capacity. Enhanced passage of Ara h 1 and Ara h 2 through the intestinal mucosa after partial digestion of PN by this *Staphylococcus* strain was also confirmed with Ussing chambers, highlighting the role of bacterial activity in systemic allergen access, a critical step in anaphylactic

reactions[45]. These results indicate that *Staphylococcus* species, including *Staphylococcus aureus,* may facilitate allergen passage through the mucosal barrier and promote allergic inflammation when allergen degradation is incomplete[66,67]. Some *Staphylococcus* strains can also compromise the epithelial barrier and increase permeability directly[68,69]. Therefore, microbes may have a dual impact on IgE-mediated immune responses, depending on the bacteria's ability to degrade PN allergens, regardless of its taxonomy. Complete microbial degradation of PN allergens reduces IgE responses, while inefficient metabolism may promote anaphylaxis by enhancing the passage of allergens through the mucosa. Altogether, the ability of the microbiota to completely degrade immunodominant allergens and reduce IgE recognition of PN significantly influences subsequent mast cell activation and anaphylactic reactions.

The primary medical recommendation for food allergic patients is strict avoidance of the allergenic food. However, this is almost an unsurmountable challenge for certain allergies, given the ubiquity of some foods such as egg, wheat, milk or PN, resulting in a high rate of accidental exposures[7,70,71]. Allergen thresholds differ among PN-allergic patients, with some individuals experiencing anaphylactic reactions even after exposure to minimal amounts of PN[72,73]. To investigate the potential role of microbial allergen metabolism in food-induced anaphylaxis, we characterized the oral microbiota of PN-allergic patients starting OIT and presenting with varying allergen thresholds. Ara h 2-specific IgE was associated with allergen thresholds, consistent with previous findings[74,75]. Interestingly, patients with higher PN threshold presented higher relative abundance of *Micrococcales*—an order including PN-degrading *Rothia* and *Micrococcus*—, than highly sensitive allergic patients to PN, independently of IgE titers. Similarly, previous studies have reported an increased relative abundance of *Rothia* in the saliva of PN-allergic children undergoing OIT[76]. Moreover, PN threshold has been linked to bacterial composition in the saliva of PN-allergic children, with *Rothia aeria*[77] and *Veillonella*[78]—oral microbiota members with PN-degrading capacity—increasing among those with greater reaction threshold. These findings suggest that the threshold of allergen reactivity correlates with the metabolic activity of oral microbiota against food allergens, potentially serving as a predictive marker for assessing allergen reactivity. Longitudinal assessment of oral microbiota and allergen reactivity during peanut OIT in future studies will further inform how microbiota may influence OIT outcomes. Although OIT remains the only allergen-specific treatment with disease-modifying potential, it is associated with limitations such as events that compromise patient adherence, quality of life, and overall effectiveness[54,79,80]. Functional analysis of the oral microbiota may help identify patients with low allergen thresholds who are unable to undergo OIT. Furthermore, the unique capacity of microorganisms to metabolize PN allergens could be leveraged to raise allergen reactivity threshold. Characterizing PN-degrading bacteria could also be applied to reduce cross-contamination risks—a leading cause of unintentional allergen exposure and a significant concern in food allergy management[71,81-83]—and improve the formulation of hypoallergenic products. In summary, our findings reveal a novel microbial mechanism of relevance in food-induced anaphylaxis. Overall, our results underscore the role of the human microbiota in dictating the severity of IgE-mediated reactions upon food

exposure through allergen metabolism and highlight the therapeutic potential of harnessing bacterial allergen-degrading capabilities for managing food allergies.

RESOURCE AVAILABILITY

Lead contact: Further information and requests for resources and reagents should be directed to the lead contact Alberto Caminero (acamine@mcmaster.ca).

Materials availability: This study did not generate new unique reagents.

Data and code availability: The microbiome sequencing data generated in this study have been deposited in the NCBI BioProject database under the accession number PRJNA1223483. The mass spectrometry proteomics data have been deposited to the ProteomeXchange Consortium via the PRIDE partner repository with the dataset identifier PXD060888 and 10.6019/PXD060888. Any additional information required to reanalyze the data reported in this paper is available from the lead contact upon reasonable request.

ACKNOWLEDGMENTS

The authors thank the staff of the Axenic & Gnotobiotic Unit at McMaster University, Dr. Heather G. Galipeau, Dr. Giada De Palma, Joe Noratangelo, Michael Rosati, and Sarah Armstrong for their assistance with mouse care. We also thank the McMaster Genome Facility, Laura Rosati, and Michelle Shah for technical support with 16S rRNA gene sequencing. We are grateful to Dr. Pablo Rodríguez del Río, Dr. Salvador Iborra and Dr. Francisco Sánchez-Madrid for their critical review of the manuscript. This work was supported by grants from The Nutricia Research Foundation (NRF-2021-13) and the New Frontiers in Research Fund (NFRFE-2019-00083) to R.J.-S. and A.C.; and by a grant from the European Food Safety Authority (GP/EFSA/ENCO/2020/02-1) to F.J.M. R.J.-S.´s laboratory is supported by the Instituto de Salud Carlos III (ISCIII; CP20/00043; PI22/00236; RD24/0007/0037) and by the Ministerio de Ciencia, Innovación y Universidades (CNS2024-154194). A.C. holds a Family Douglas Research Chair in Intestinal Research and is funded by the Canadian Institutes of Health Research (CIHR; Project Grant 202010PJT), NSERC (DGECR-2022-00221) and by Crohn's and Colitis Canada (CCC, Grants-In-Aid grant). L.E.R. is supported by a Frederick Banting and Charles Best Canada Graduate Scholarship-Doctoral award from CIHR and a graduate scholarship from the Farncombe Family Digestive Health Research Institute. E.S.-M. is supported by a Formación de Profesorado Universitario grant (FPU23/03341) from Ministerio de Universidades. S.U.P. is supported by NIAID NIH R01 grants 1R01aI155630 and 1R01AI182001. L.M.-S. is supported by the Investigo program through the Ministerio de Trabajo y Economía Social, Servicio Público de Empleo (SEPE), which is funded by "Plan de Recuperación, Transformación y Resiliencia" and "NextGenerationEU" of the

European Union (2022- C23.I01). C.L.S and E.N.-B are supported by a Río Hortega (CM23/0019) and a Sara Borrell grant (CD23/00125), respectively, from ISCIII. E.F.V. is supported by a CIHR Project Grant (PJT-183881) and holds a Tier 1 Canada Research Chair in Microbial Therapeutics and Nutrition in Gastroenterology.

AUTHOR CONTRIBUTIONS

Conceptualization, R.J.-S., A.C.; Methodology, R.J.-S., A.C.; Investigation, E.S.-M., L.E.R., M.G.-R., D.H., P.H., B.B., G.Y., R.D., J.F.E.K., T.D.W., L.M.-S., C.L.S., E.N.-B., X.Y.W., F.J.M., R.J.-S., A.C.; Resources, M.G.-A., A.D.-P., E.F.V., Y.R.C., P.O., F.V., C.B., J.F.E.K, M.J., W.G.S., S.U.P., F.J.M., M.G.S.; Writing – Original Draft Preparation, E.S.-M., L.E.R., R.J.-S., A.C.; Writing – Review & Editing Preparation, E.S.-M., L.E.R., R.J.-S., A.C.; Visualization Preparation, E.S.-M., L.E.R.; Supervision, R.J.-S., A.C.; funding Acquisition, R.J.-S., A.C.

DECLARATION OF INTERESTS

R.J.-S. receives research funds from a collaboration agreement between FIB-Hospital Universitario de La Princesa and Inmunotek S.L., which does not present any conflicts with the data presented. Provisional patent (63/670,312) was filed in the United States Patent and Trademark office based on data presented in this manuscript (“Microbial metabolism of peanut allergens and uses thereof).

SUPPLEMENTAL INFORMATION INDEX

Figures S1-S5 and their legends, as well as Tables S1 and S2 are in a PDF.

References

1. Meizlish, M.L., Franklin, R.A., Zhou, X., and Medzhitov, R. (2021). Tissue Homeostasis and Inflammation. Annu Rev Immunol *39*, 557-581. 10.1146/annurev-immunol-061020-053734.
2. Galli, S.J., and Tsai, M. (2012). IgE and mast cells in allergic disease. Nat Med *18*, 693-704. 10.1038/nm.2755.
3. Nunez-Borque, E., Dribin, T.E., Rodriguez Del Rio, P., Camargo, C.A., Jr., Esteban, V., du Toit, G., Jimenez-Saiz, R., and Giovannini, M. (2025). Anaphylaxis: Spotlight on Inflammation. Clin Exp Allergy *55*, 8-10. 10.1111/cea.14610.
4. Dyer, A.A., Rivkina, V., Perumal, D., Smeltzer, B.M., Smith, B.M., and Gupta, R.S. (2015). Epidemiology of childhood peanut allergy. Allergy Asthma Proc *36*, 58-64. 10.2500/aap.2015.36.3819.
5. Cianferoni, A., and Muraro, A. (2012). Food-induced anaphylaxis. Immunol Allergy Clin North Am *32*, 165-195. 10.1016/j.iac.2011.10.002.
6. Neuman-Sunshine, D.L., Eckman, J.A., Keet, C.A., Matsui, E.C., Peng, R.D., Lenehan, P.J., and Wood, R.A. (2012). The natural history of persistent peanut allergy. Ann Allergy Asthma Immunol *108*, 326-331 e323. 10.1016/j.anai.2011.11.010.
7. Cherkaoui, S., Ben-Shoshan, M., Alizadehfar, R., Asai, Y., Chan, E., Cheuk, S., Shand, G., St-Pierre, Y., Harada, L., Allen, M., and Clarke, A. (2015). Accidental exposures to peanut in a large cohort of Canadian children with peanut allergy. Clin Transl Allergy *5*, 16. 10.1186/s13601-015-0055-x.
8. Peters, R.L., Guarnieri, I., Tang, M.L.K., Lowe, A.J., Dharmage, S.C., Perrett, K.P., Gurrin, L.C., and Koplin, J.J. (2022). The natural history of peanut and egg allergy in children up to age 6 years in the HealthNuts population-based longitudinal study. J Allergy Clin Immunol *150*, 657-665 e613. 10.1016/j.jaci.2022.04.008.
9. Benede, S., Garrido-Arandia, M., Martin-Pedraza, L., Bueno, C., Diaz-Perales, A., and Villalba, M. (2017). Multifactorial Modulation of Food-Induced Anaphylaxis. Front Immunol *8*, 552. 10.3389/fimmu.2017.00552.
10. Munoz-Cano, R., Pascal, M., Araujo, G., Goikoetxea, M.J., Valero, A.L., Picado, C., and Bartra, J. (2017). Mechanisms, Cofactors, and Augmenting Factors Involved in Anaphylaxis. Front Immunol *8*, 1193. 10.3389/fimmu.2017.01193.
11. Flinn, A., and Hourihane, J.O. (2013). Allergic reaction to peanuts: can we predict reaction severity in the wild? Curr Allergy Asthma Rep *13*, 645-650. 10.1007/s11882-013-0369-5.
12. Petek, T., Lajhar, M., Krasovec, B., Homsak, M., Kavalar, M., Korosec, P., Koren, B., Tomazin, M., Hojnik, T., and Berce, V. (2023). Risk Factors for Anaphylaxis in Children Allergic to Peanuts. Medicina (Kaunas) *59*. 10.3390/medicina59061037.
13. Turner, P.J., Baumert, J.L., Beyer, K., Boyle, R.J., Chan, C.H., Clark, A.T., Crevel, R.W., DunnGalvin, A., Fernandez-Rivas, M., Gowland, M.H., et al. (2016). Can we identify patients at risk of life-threatening allergic reactions to food? Allergy *71*, 1241-1255. 10.1111/all.12924.

14. Caminero, A., Meisel, M., Jabri, B., and Verdu, E.F. (2019). Mechanisms by which gut microorganisms influence food sensitivities. Nat Rev Gastroenterol Hepatol *16*, 7-18. 10.1038/s41575-018-0064-z.
15. Stephen-Victor, E., Crestani, E., and Chatila, T.A. (2020). Dietary and Microbial Determinants in Food Allergy. Immunity *53*, 277-289. 10.1016/j.immuni.2020.07.025.
16. Cerovic, V., Pabst, O., and Mowat, A.M. (2025). The renaissance of oral tolerance: merging tradition and new insights. Nat Rev Immunol *25*, 42-56. 10.1038/s41577-024-01077-7.
17. Stephen-Victor, E., Kuziel, G.A., Martinez-Blanco, M., Jugder, B.E., Benamar, M., Wang, Z., Chen, Q., Lozano, G.L., Abdel-Gadir, A., Cui, Y., et al. (2025). RELMbeta sets the threshold for microbiome-dependent oral tolerance. Nature. 10.1038/s41586-024-08440-7.
18. Azad, M.B., Konya, T., Guttman, D.S., Field, C.J., Sears, M.R., HayGlass, K.T., Mandhane, P.J., Turvey, S.E., Subbarao, P., Becker, A.B., et al. (2015). Infant gut microbiota and food sensitization: associations in the first year of life. Clin Exp Allergy *45*, 632-643. 10.1111/cea.12487.
19. De Filippis, F., Paparo, L., Nocerino, R., Della Gatta, G., Carucci, L., Russo, R., Pasolli, E., Ercolini, D., and Berni Canani, R. (2021). Specific gut microbiome signatures and the associated pro-inflamatory functions are linked to pediatric allergy and acquisition of immune tolerance. Nature Communications *12*. 10.1038/s41467-021-26266-z.
20. Bao, R., Hesser, L.A., He, Z., Zhou, X., Nadeau, K.C., and Nagler, C.R. (2021). Fecal microbiome and metabolome differ in healthy and food-allergic twins. J Clin Invest *131*. 10.1172/JCI141935.
21. Koppelman, S.J., Hefle, S.L., Taylor, S.L., and de Jong, G.A. (2010). Digestion of peanut allergens Ara h 1, Ara h 2, Ara h 3, and Ara h 6: a comparative in vitro study and partial characterization of digestion-resistant peptides. Mol Nutr Food Res *54*, 1711-1721. 10.1002/mnfr.201000011.
22. Kopper, R.A., Odum, N.J., Sen, M., Helm, R.M., Steve Stanley, J., and Wesley Burks, A. (2004). Peanut protein allergens: gastric digestion is carried out exclusively by pepsin. J Allergy Clin Immunol *114*, 614-618. 10.1016/j.jaci.2004.05.012.
23. Jimenez-Saiz, R., Benede, S., Molina, E., and Lopez-Exposito, I. (2015). Effect of processing technologies on the allergenicity of food products. Critical reviews in food science and nutrition *55*, 1902-1917. 10.1080/10408398.2012.736435.
24. Moreno, F.J. (2007). Gastrointestinal digestion of food allergens: effect on their allergenicity. Biomed Pharmacother *61*, 50-60. 10.1016/j.biopha.2006.10.005.
25. Gertie, J.A., Zhang, B., Liu, E.G., Hoyt, L.R., Yin, X., Xu, L., Long, L.L., Soldatenko, A., Gowthaman, U., Williams, A., and Eisenbarth, S.C. (2022). Oral anaphylaxis to peanut in a mouse model is associated with gut permeability but not with Tlr4 or Dock8 mutations. J Allergy Clin Immunol *149*, 262-274. 10.1016/j.jaci.2021.05.015.
26. Whelan, F.J., Waddell, B., Syed, S.A., Shekarriz, S., Rabin, H.R., Parkins, M.D., and Surette, M.G. (2020). Culture-enriched metagenomic sequencing enables in-

depth profiling of the cystic fibrosis lung microbiota. Nat Microbiol *5*, 379-390. 10.1038/s41564-019-0643-y.

27. Tsilochristou, O., du Toit, G., Sayre, P.H., Roberts, G., Lawson, K., Sever, M.L., Bahnson, H.T., Radulovic, S., Basting, M., Plaut, M., et al. (2019). Association of Staphylococcus aureus colonization with food allergy occurs independently of eczema severity. J Allergy Clin Immunol *144*, 494-503. 10.1016/j.jaci.2019.04.025.
28. Koppelman, S.J., Vlooswijk, R.A., Knippels, L.M., Hessing, M., Knol, E.F., van Reijsen, F.C., and Bruijnzeel-Koomen, C.A. (2001). Quantification of major peanut allergens Ara h 1 and Ara h 2 in the peanut varieties Runner, Spanish, Virginia, and Valencia, bred in different parts of the world. Allergy *56*, 132-137. 10.1034/j.1398-9995.2001.056002132.x.
29. Jiang, S., Wang, S., Sun, Y., Zhou, Z., and Wang, G. (2011). Molecular characterization of major allergens Ara h 1, 2, 3 in peanut seed. Plant Cell Rep *30*, 1135-1143. 10.1007/s00299-011-1022-1.
30. Burks, A.W., Shin, D., Cockrell, G., Stanley, J.S., Helm, R.M., and Bannon, G.A. (1997). Mapping and mutational analysis of the IgE-binding epitopes on Ara h 1, a legume vicilin protein and a major allergen in peanut hypersensitivity. Eur J Biochem *245*, 334-339. 10.1111/j.1432-1033.1997.t01-1-00334.x.
31. Shin, D.S., Compadre, C.M., Maleki, S.J., Kopper, R.A., Sampson, H., Huang, S.K., Burks, A.W., and Bannon, G.A. (1998). Biochemical and structural analysis of the IgE binding sites on ara h1, an abundant and highly allergenic peanut protein. J Biol Chem *273*, 13753-13759. 10.1074/jbc.273.22.13753.
32. Lopez-Sanz, C., Sanchez-Martinez, E., and Jimenez-Saiz, R. (2022). Protocol to desensitize human and murine mast cells after polyclonal IgE sensitization. STAR Protoc *3*, 101755. 10.1016/j.xpro.2022.101755.
33. Fernandez-Gallego, N., Castillo-Gonzalez, R., Moreno-Serna, L., Garcia-Civico, A.J., Sanchez-Martinez, E., Lopez-Sanz, C., Fontes, A.L., Pimentel, L.L., Gradillas, A., Obeso, D., et al. (2024). Allergic inflammation triggers dyslipidemia via IgG signalling. Allergy *79*, 2680-2699. 10.1111/all.16187.
34. Gomez de Aguero, M., Ganal-Vonarburg, S.C., Fuhrer, T., Rupp, S., Uchimura, Y., Li, H., Steinert, A., Heikenwalder, M., Hapfelmeier, S., Sauer, U., et al. (2016). The maternal microbiota drives early postnatal innate immune development. Science *351*, 1296-1302. 10.1126/science.aad2571.
35. Caminero, A., Guzman, M., Libertucci, J., and Lomax, A.E. (2023). The emerging roles of bacterial proteases in intestinal diseases. Gut Microbes *15*, 2181922. 10.1080/19490976.2023.2181922.
36. Shan, L., Molberg, O., Parrot, I., Hausch, F., Filiz, F., Gray, G.M., Sollid, L.M., and Khosla, C. (2002). Structural basis for gluten intolerance in celiac sprue. Science *297*, 2275-2279. 10.1126/science.1074129.
37. Caminero, A., Galipeau, H.J., McCarville, J.L., Johnston, C.W., Bernier, S.P., Russell, A.K., Jury, J., Herran, A.R., Casqueiro, J., Tye-Din, J.A., et al. (2016). Duodenal Bacteria From Patients With Celiac Disease and Healthy Subjects Distinctly Affect Gluten Breakdown and Immunogenicity. Gastroenterology *151*, 670-683. 10.1053/j.gastro.2016.06.041.

38. Caminero, A., McCarville, J.L., Zevallos, V.F., Pigrau, M., Yu, X.B., Jury, J., Galipeau, H.J., Clarizio, A.V., Casqueiro, J., Murray, J.A., et al. (2019). Lactobacilli Degrade Wheat Amylase Trypsin Inhibitors to Reduce Intestinal Dysfunction Induced by Immunogenic Wheat Proteins. Gastroenterology *156*, 2266-2280. 10.1053/j.gastro.2019.02.028.
39. Tremaroli, V., and Backhed, F. (2012). Functional interactions between the gut microbiota and host metabolism. Nature *489*, 242-249. 10.1038/nature11552.
40. Thomson, C.A., Morgan, S.C., Ohland, C., and McCoy, K.D. (2022). From germ-free to wild: modulating microbiome complexity to understand mucosal immunology. Mucosal Immunol *15*, 1085-1094. 10.1038/s41385-022-00562-3.
41. Jimenez-Saiz, R., Anipindi, V.C., Galipeau, H., Ellenbogen, Y., Chaudhary, R., Koenig, J.F., Gordon, M.E., Walker, T.D., Mandur, T.S., Abed, S., et al. (2020). Microbial Regulation of Enteric Eosinophils and Its Impact on Tissue Remodeling and Th2 Immunity. Front Immunol *11*, 155. 10.3389/fimmu.2020.00155.
42. Jutel, M., Agache, I., Zemelka-Wiacek, M., Akdis, M., Chivato, T., Del Giacco, S., Gajdanowicz, P., Gracia, I.E., Klimek, L., Lauerma, A., et al. (2023). Nomenclature of allergic diseases and hypersensitivity reactions: Adapted to modern needs: An EAACI position paper. Allergy *78*, 2851-2874. 10.1111/all.15889.
43. Leyva-Castillo, J.M., Galand, C., Kam, C., Burton, O., Gurish, M., Musser, M.A., Goldsmith, J.D., Hait, E., Nurko, S., Brombacher, F., et al. (2019). Mechanical Skin Injury Promotes Food Anaphylaxis by Driving Intestinal Mast Cell Expansion. Immunity *50*, 1262-1275 e1264. 10.1016/j.immuni.2019.03.023.
44. Jacob, C., Yang, P.C., Darmoul, D., Amadesi, S., Saito, T., Cottrell, G.S., Coelho, A.M., Singh, P., Grady, E.F., Perdue, M., and Bunnett, N.W. (2005). Mast cell tryptase controls paracellular permeability of the intestine. Role of protease-activated receptor 2 and beta-arrestins. J Biol Chem *280*, 31936-31948. 10.1074/jbc.M506338200.
45. Strait, R.T., Mahler, A., Hogan, S., Khodoun, M., Shibuya, A., and Finkelman, F.D. (2011). Ingested allergens must be absorbed systemically to induce systemic anaphylaxis. J Allergy Clin Immunol *127*, 982-989 e981. 10.1016/j.jaci.2011.01.034.
46. Cahenzli, J., Koller, Y., Wyss, M., Geuking, M.B., and McCoy, K.D. (2013). Intestinal microbial diversity during early-life colonization shapes long-term IgE levels. Cell Host Microbe *14*, 559-570. 10.1016/j.chom.2013.10.004.
47. Wyss, M., Brown, K., Thomson, C.A., Koegler, M., Terra, F., Fan, V., Ronchi, F., Bihan, D., Lewis, I., Geuking, M.B., and McCoy, K.D. (2019). Using Precisely Defined in vivo Microbiotas to Understand Microbial Regulation of IgE. Front Immunol *10*, 3107. 10.3389/fimmu.2019.03107.
48. Stefka, A.T., Feehley, T., Tripathi, P., Qiu, J., McCoy, K., Mazmanian, S.K., Tjota, M.Y., Seo, G.Y., Cao, S., Theriault, B.R., et al. (2014). Commensal bacteria protect against food allergen sensitization. Proc Natl Acad Sci U S A *111*, 13145-13150. 10.1073/pnas.1412008111.
49. Arias, K., Chu, D.K., Flader, K., Botelho, F., Walker, T., Arias, N., Humbles, A.A., Coyle, A.J., Oettgen, H.C., Chang, H.D., et al. (2011). Distinct immune effector pathways contribute to the full expression of peanut-induced anaphylactic

reactions in mice. J Allergy Clin Immunol *127*, 1552-1561 e1551. 10.1016/j.jaci.2011.03.044.

50. Gowthaman, U., Chen, J.S., Zhang, B., Flynn, W.F., Lu, Y., Song, W., Joseph, J., Gertie, J.A., Xu, L., Collet, M.A., et al. (2019). Identification of a T follicular helper cell subset that drives anaphylactic IgE. Science *365*, eaaw6433. 10.1126/science.aaw6433.
51. Chu, D.K., Jimenez-Saiz, R., Verschoor, C.P., Walker, T.D., Goncharova, S., Llop-Guevara, A., Shen, P., Gordon, M.E., Barra, N.G., Bassett, J.D., et al. (2014). Indigenous enteric eosinophils control DCs to initiate a primary Th2 immune response in vivo. J Exp Med *211*, 1657-1672. 10.1084/jem.20131800.
52. Jimenez-Saiz, R., Chu, D.K., Mandur, T.S., Walker, T.D., Gordon, M.E., Chaudhary, R., Koenig, J., Saliba, S., Galipeau, H.J., Utley, A., et al. (2017). Lifelong memory responses perpetuate humoral T(H)2 immunity and anaphylaxis in food allergy. J Allergy Clin Immunol *140*, 1604-1615 e1605. 10.1016/j.jaci.2017.01.018.
53. Knibb, R.C., Jones, C.J., Herbert, L.J., and Screti, C. (2024). Psychological support needs for children with food allergy and their families: A systematic review. Pediatr Allergy Immunol *35*, e14108. 10.1111/pai.14108.
54. Mori, F., Giovannini, M., Barni, S., Jimenez-Saiz, R., Munblit, D., Biagioni, B., Liccioli, G., Sarti, L., Liotti, L., Ricci, S., et al. (2021). Oral Immunotherapy for Food-Allergic Children: A Pro-Con Debate. Front Immunol *12*, 636612. 10.3389/fimmu.2021.636612.
55. Niggemann, B., and Beyer, K. (2014). Factors augmenting allergic reactions. Allergy *69*, 1582-1587. 10.1111/all.12532.
56. Piletta-Zanin, A., Scherl, A., Benhamou, A., Braendle, G., Caubet, J.C., Graham, F., Grosgurin, O., Harr, T., Manzano, S., Nigolian, H., et al. (2025). The Severity of Allergic Reactions in a Real-World Environment Is Independent of the Eliciting Amounts of Foods. Allergy *80*, 238-247. 10.1111/all.16413.
57. Baker, J.L., Mark Welch, J.L., Kauffman, K.M., McLean, J.S., and He, X. (2024). The oral microbiome: diversity, biogeography and human health. Nat Rev Microbiol *22*, 89-104. 10.1038/s41579-023-00963-6.
58. Constante, M., Libertucci, J., Galipeau, H.J., Szamosi, J.C., Rueda, G., Miranda, P.M., Pinto-Sanchez, M.I., Southward, C.M., Rossi, L., Fontes, M.E., et al. (2022). Biogeographic Variation and Functional Pathways of the Gut Microbiota in Celiac Disease. Gastroenterology *163*, 1351-1363 e1315. 10.1053/j.gastro.2022.06.088.
59. Kunath, B.J., De Rudder, C., Laczny, C.C., Letellier, E., and Wilmes, P. (2024). The oral-gut microbiome axis in health and disease. Nat Rev Microbiol *22*, 791-805. 10.1038/s41579-024-01075-5.
60. Zamakhchari, M., Wei, G., Dewhirst, F., Lee, J., Schuppan, D., Oppenheim, F.G., and Helmerhorst, E.J. (2011). Identification of Rothia bacteria as gluten-degrading natural colonizers of the upper gastro-intestinal tract. PLoS One *6*, e24455. 10.1371/journal.pone.0024455.
61. Wei, G., Tian, N., Siezen, R., Schuppan, D., and Helmerhorst, E.J. (2016). Identification of food-grade subtilisins as gluten-degrading enzymes to treat

celiac disease. Am J Physiol Gastrointest Liver Physiol *311*, G571-580. 10.1152/ajpgi.00185.2016.

62. Patrick, G.J., Liu, H., Alphonse, M.P., Dikeman, D.A., Youn, C., Otterson, J.C., Wang, Y., Ravipati, A., Mazhar, M., Denny, G., et al. (2021). Epicutaneous Staphylococcus aureus induces IL-36 to enhance IgE production and ensuing allergic disease. J Clin Invest *131*. 10.1172/JCI143334.
63. Rondeau, L.E., Da Luz, B.B., Santiago, A., Bermudez-Brito, M., Hann, A., De Palma, G., Jury, J., Wang, X., Verdu, E.F., Galipeau, H.J., et al. (2024). Proteolytic bacteria expansion during colitis amplifies inflammation through cleavage of the external domain of PAR2. Gut Microbes *16*, 2387857. 10.1080/19490976.2024.2387857.
64. Agaronyan, K., Sharma, L., Vaidyanathan, B., Glenn, K., Yu, S., Annicelli, C., Wiggen, T.D., Penningroth, M.R., Hunter, R.C., Dela Cruz, C.S., and Medzhitov, R. (2022). Tissue remodeling by an opportunistic pathogen triggers allergic inflammation. Immunity *55*, 895-911 e810. 10.1016/j.immuni.2022.04.001.
65. Caminero, A., McCarville, J.L., Galipeau, H.J., Deraison, C., Bernier, S.P., Constante, M., Rolland, C., Meisel, M., Murray, J.A., Yu, X.B., et al. (2019). Duodenal bacterial proteolytic activity determines sensitivity to dietary antigen through protease-activated receptor-2. Nat Commun *10*, 1198. 10.1038/s41467-019-09037-9.
66. Jimenez-Saiz, R., Ellenbogen, Y., Koenig, J.F.E., Gordon, M.E., Walker, T.D., Rosace, D., Spill, P., Bruton, K., Kong, J., Monteiro, K., et al. (2019). IgG1(+) B-cell immunity predates IgE responses in epicutaneous sensitization to foods. Allergy *74*, 165-175. 10.1111/all.13481.
67. Kong, J., Chalcraft, K., Mandur, T.S., Jimenez-Saiz, R., Walker, T.D., Goncharova, S., Gordon, M.E., Naji, L., Flader, K., Larche, M., et al. (2015). Comprehensive metabolomics identifies the alarmin uric acid as a critical signal for the induction of peanut allergy. Allergy *70*, 495-505. 10.1111/all.12579.
68. Kwak, Y.K., Vikstrom, E., Magnusson, K.E., Vecsey-Semjen, B., Colque-Navarro, P., and Mollby, R. (2012). The Staphylococcus aureus alpha-toxin perturbs the barrier function in Caco-2 epithelial cell monolayers by altering junctional integrity. Infect Immun *80*, 1670-1680. 10.1128/IAI.00001-12.
69. Moran, M.C., Brewer, M.G., Schlievert, P.M., and Beck, L.A. (2023). S. aureus virulence factors decrease epithelial barrier function and increase susceptibility to viral infection. Microbiol Spectr *11*, e0168423. 10.1128/spectrum.01684-23.
70. Rotella, K., and Oriel, R.C. (2022). Accidental Reactions to Foods: Frequency, Causes, and Severity. Curr Treat Options Allergy *9*, 157-168. 10.1007/s40521-022-00314-5.
71. Hsu, C., Hosakoppal, S., Yong, M., Gupta, R., Makhija, M., and Singh, A.M. (2024). Prevalence and Characteristics of Accidental Ingestions Among Pediatric Food Allergy Patients. J Allergy Clin Immunol Pract *12*, 3089-3095 e3082. 10.1016/j.jaip.2024.08.006.
72. Li, J.C., Rotter, N.S., Stieb, E.S., Stockbridge, J.L., Theodorakakis, M.D., and Shreffler, W.G. (2024). Utility of food allergy thresholds. Ann Allergy Asthma Immunol *132*, 321-327. 10.1016/j.anai.2023.12.012.

73. Patel, N., Adelman, D.C., Anagnostou, K., Baumert, J.L., Blom, W.M., Campbell, D.E., Chinthrajah, R.S., Mills, E.N.C., Javed, B., Purington, N., et al. (2021). Using data from food challenges to inform management of consumers with food allergy: A systematic review with individual participant data meta-analysis. J Allergy Clin Immunol *147*, 2249-2262 e2247. 10.1016/j.jaci.2021.01.025.
74. Santos, A.F., Barbosa-Morais, N.L., Hurlburt, B.K., Ramaswamy, S., Hemmings, O., Kwok, M., O'Rourke, C., Bahnson, H.T., Cheng, H., James, L., et al. (2020). IgE to epitopes of Ara h 2 enhance the diagnostic accuracy of Ara h 2-specific IgE. Allergy *75*, 2309-2318. 10.1111/all.14301.
75. Patil, S.U., Steinbrecher, J., Calatroni, A., Smith, N., Ma, A., Ruiter, B., Virkud, Y., Schneider, M., and Shreffler, W.G. (2019). Early decrease in basophil sensitivity to Ara h 2 precedes sustained unresponsiveness after peanut oral immunotherapy. J Allergy Clin Immunol *144*, 1310-1319 e1314. 10.1016/j.jaci.2019.07.028.
76. Blackman, A.C., Thapa, S., Venkatachalam, A., Horvath, T.D., Runge, J.K., Haidacher, S.J., Hoch, K.M., Haag, A.M., Luna, R.A., and Anagnostou, A. (2022). Insights into Microbiome and Metabolic Signatures of Children Undergoing Peanut Oral Immunotherapy. Children (Basel) *9*. 10.3390/children9081192.
77. Zhang, L., Chun, Y., Grishina, G., Lo, T., Reed, K., Wang, J., Sicherer, S., Berin, M.C., and Bunyavanich, S. (2025). Oral and Gut Microbial Hubs Associated With Reaction Threshold Interact With Circulating Immune Factors in Peanut Allergy. Allergy *n/a*. 10.1111/all.16481.
78. Zhang, L., Chun, Y., Ho, H.E., Arditi, Z., Lo, T., Sajja, S., Rose, R., Jones, D., Wang, J., Sicherer, S., and Bunyavanich, S. (2022). Multiscale study of the oral and gut environments in children with high- and low-threshold peanut allergy. J Allergy Clin Immunol *150*, 714-720 e712. 10.1016/j.jaci.2022.04.026.
79. Chu, D.K., Wood, R.A., French, S., Fiocchi, A., Jordana, M., Waserman, S., Brozek, J.L., and Schunemann, H.J. (2019). Oral immunotherapy for peanut allergy (PACE): a systematic review and meta-analysis of efficacy and safety. Lancet *393*, 2222-2232. 10.1016/S0140-6736(19)30420-9.
80. Barshow, S., Tirumalasetty, J., Sampath, V., Zhou, X., Seastedt, H., Schuetz, J., and Nadeau, K. (2024). The Immunobiology and Treatment of Food Allergy. Annu Rev Immunol *42*, 401-425. 10.1146/annurev-immunol-090122-043501.
81. Fierstein, J.L., Brown, D., Gupta, R., and Bilaver, L. (2021). Understanding Food-Related Allergic Reactions Through a US National Patient Registry. J Allergy Clin Immunol Pract *9*, 206-215 e201. 10.1016/j.jaip.2020.08.011.
82. Taylor, S.L., and Baumert, J.L. (2010). Cross-contamination of foods and implications for food allergic patients. Curr Allergy Asthma Rep *10*, 265-270. 10.1007/s11882-010-0112-4.
83. Miller, T.A., Koppelman, S.J., Bird, J.A., Hernandez-Trujillo, V., Thyagarajan, A., Mack, D., Chalil, J.M., Green, T.D., and Baumert, J.L. (2022). Peanut cross-contamination in randomly selected baked goods. Ann Allergy Asthma Immunol *128*, 439-442. 10.1016/j.anai.2022.01.037.
84. Dewhirst, F.E., Chien, C.C., Paster, B.J., Ericson, R.L., Orcutt, R.P., Schauer, D.B., and Fox, J.G. (1999). Phylogeny of the defined murine microbiota: altered

Schaedler flora. Appl Environ Microbiol *65*, 3287-3292. 10.1128/AEM.65.8.3287-3292.1999.

85. Burton, O.T., Stranks, A.J., Tamayo, J.M., Koleoglou, K.J., Schwartz, L.B., and Oettgen, H.C. (2017). A humanized mouse model of anaphylactic peanut allergy. J Allergy Clin Immunol *139*, 314-322 e319. 10.1016/j.jaci.2016.04.034.
86. Whelan, F.J., and Surette, M.G. (2017). A comprehensive evaluation of the sl1p pipeline for 16S rRNA gene sequencing analysis. Microbiome *5*, 100. 10.1186/s40168-017-0314-2.
87. Pazos-Castro, D., Gonzalez-Klein, Z., Montalvo, A.Y., Hernandez-Ramirez, G., Romero-Sahagun, A., Esteban, V., Garrido-Arandia, M., Tome-Amat, J., and Diaz-Perales, A. (2022). NLRP3 priming due to skin damage precedes LTP allergic sensitization in a mouse model. Sci Rep *12*, 3329. 10.1038/s41598-022-07421-y.
88. Wang, Y., Matsushita, K., Jackson, J., Numata, T., Zhang, Y., Zhou, G., Tsai, M., and Galli, S.J. (2021). Transcriptome programming of IL-3-dependent bone marrow-derived cultured mast cells by stem cell factor (SCF). Allergy *76*, 2288-2291. 10.1111/all.14808.
89. Kechin, A., Boyarskikh, U., Kel, A., and Filipenko, M. (2017). cutPrimers: A New Tool for Accurate Cutting of Primers from Reads of Targeted Next Generation Sequencing. J Comput Biol *24*, 1138-1143. 10.1089/cmb.2017.0096.
90. Martin, M. (2011). Cutadapt removes adapter sequences from high-througput sequencing reads. EMBnet.journal *17*, 10-12. https://doi.org/10.14806/ej.17.1.200.
91. Callahan, B.J., McMurdie, P.J., Rosen, M.J., Han, A.W., Johnson, A.J., and Holmes, S.P. (2016). DADA2: High-resolution sample inference from Illumina amplicon data. Nat Methods *13*, 581-583. 10.1038/nmeth.3869.
92. Quast, C., Pruesse, E., Yilmaz, P., Gerken, J., Schweer, T., Yarza, P., Peplies, J., and Glockner, F.O. (2013). The SILVA ribosomal RNA gene database project: improved data processing and web-based tools. Nucleic Acids Res *41*, D590-596. 10.1093/nar/gks1219.
93. Price, M.N., Dehal, P.S., and Arkin, A.P. (2010). FastTree 2--approximately maximum-likelihood trees for large alignments. PLoS One *5*, e9490. 10.1371/journal.pone.0009490.
94. McMurdie, P.J., and Holmes, S. (2013). phyloseq: an R package for reproducible interactive analysis and graphics of microbiome census data. PLoS One *8*, e61217. 10.1371/journal.pone.0061217.

RESOURCE AVAILABILITY

Lead contact

Requests for further information or resources should be directed to the lead contact Alberto Caminero (acamine@mcmaster.ca).

Materials availability

This study did not generate new unique reagents.

Data and code availability

The microbiome sequencing data generated in this study have been deposited in the NCBI BioProject database under the accession number PRJNA1223483. The mass spectrometry proteomics data have been deposited to the ProteomeXchange Consortium via the PRIDE partner repository with the dataset identifier PXD060888 and 10.6019/PXD060888.

EXPERIMENTAL MODEL AND STUDY PARTICIPANT DETAILS

Human samples

Human saliva from peanut (PN) allergic patients entering oral immunotherapy (OIT; n=19) were collected. These samples were obtained from children aged 1-14 years who participated in a standard clinical oral food challenge to establish peanut threshold prior to clinical management with PN OIT at Massachusetts General Hospital. Saliva was collected with the SalivaBio Children's Swab (Salimetrics) following the manufacturer's protocol, and samples were stored at -80^{o}C until further use. PN- and antigen-specific Ig levels in plasma from patients undergoing OIT were measured using a Phadia ImmunoCAP 1000 instrument (ThermoFisher) according to the manufacturer's instructions. Saliva samples from healthy volunteers (n=13) were collected at McMaster University under BUP#423. All patients and healthy volunteers provided written informed consent as per local institutional review board guidelines. Supportive and demographics data can be found in Table S1.

Human sera for western blotting were provided by the Allergology Service at Hospital Universitario de La Princesa (Madrid, Spain). The Research Ethics Committee of Hospital Universitario de La Princesa approved the study protocol (reference 4460). All the donors provided written informed consent with no conflict of interest. Donor sera characterization is detailed in Supplementary Table S2.

Mice

Age-, sex-, and strain-matched controls were used in all experiments. Specific pathogen-free (SPF) C57BL/6 mice were purchased from Charles River and Taconic, while SPF C3H-HeN mice were purchased from Taconic. Germ-free (GF) C57BL/6 mice used for colonization experiments were originally purchased from Taconic and derived GF by two-stage embryo transfer. They were bred in flexible-film gnotobiotic isolators at McMaster University's Farncombe Family Digestive Health Research Institute Axenic Gnotobiotic Unit (AGU). C3H-HeN mice with altered Schaedler flora (ASF) microbiota, a simple and stable microbiota[63,84], were bred and housed in GF conditions at the AGU. All mice were maintained on a 12-h light-dark cycle and fed an autoclaved chow diet and sterile water *ad libitum*. Eight-to-12-week-old mice were used throughout. All procedures were approved by the Environmental Council of the Community of Madrid with PROEX references 45.2/20 and 9.7/23, and the McMaster University Animal Care Committee and McMaster University Animal Research Ethics Board in accordance with the Animal Utilization Protocol #22-26. Ethical regulations for animal research were strictly followed.

Food allergy and anaphylaxis model

To study the impact of microbes on PN metabolism and anaphylaxis, C3H-HeN mice with different microbiota were sensitized to PN using distinct techniques. 1. Intra-gastric sensitization: mice were provided 3.25 mg of crude PN extract (CPE; Greer Laboratories Inc) and 0.625 µg of cholera toxin (List Biological Laboratories) in 0.1 mL of PBS by oral gavage once a week for 6 weeks; 2. Intra-peritoneal sensitization: mice were provided 3.25 mg of CPE and 6.25 µg of cholera toxin in 0.1 mL of PBS intra-peritoneally once a week for 4 weeks; 3. Passive sensitization- mice were subjected to 3 intra-peritoneal injections (0.1, 0.2, and 0.4 mL) of serum obtained from intra-peritoneally sensitized PN-allergic mice as described[33]. After sensitization, mice were challenged with a 24 mg bolus of CPE in 0.8 mL of PBS by oral gavage. In some experiments, CPE was pre-digested with PN allergen-degrading bacteria (*Rothia* R1, *Staphylococcus* S1, or S2), or mice were colonized with PN-degrading bacteria (*Rothia* R1, R2, and R3), prior to the oral challenge to evaluate the impact of bacterial PN metabolism on allergenicity and anaphylaxis. Serum was collected 48 h before challenge. Mice were monitored for 40 min after challenge for changes in rectal (core) body temperature. Peripheral blood was collected, and mice were euthanized 40 min after the oral challenge. Mucosal mast cell protease 1 (mMCP-1) was quantified in serum after the PN challenge, as it is a key biomarker of anaphylaxis in mice, serving a similar role to serum tryptase for indicating mast cell activation in humans[85].

Microbiota model for studying microbial PN metabolism

To investigate the role of microbiota in PN metabolism, we used two colonization approaches: 1. We studied PN metabolism in mice colonized with ASF and SPF microbiota, and GF controls; 2. GF C57BL/6 mice were mono-colonized with selected PN-degrading bacteria (*Rothia* R3 or *Staphylococcus* S1, S2, or S3). After colonization,

mice were administered 24 mg of CPE in 0.8 mL of PBS by oral gavage. Small and large intestinal contents and serum from peripheral blood were collected 40 minutes post-administration for quantification of PN allergens Ara h 1 and Ara h 2 in biological samples by ELISA (Indoor Biotechnologies) as described below. Additionally, small intestinal contents were incubated *ex vivo* with CPE overnight (o/n), and remaining Ara h 1 and Ara h 2 levels were quantified by ELISA (Indoor Biotechnologies).

Characterization of bacterial PN-degradation and immune activation

To assess bacterial degradation of PN allergens and its impact on immune activation, we performed *in vitro* digestions, proteomic characterization, and mast cell activation assays. Bacterial isolates were incubated with CPE and degradation of Ara h 1 and Ara h 2 was quantified by ELISA. Then, *Rothia* (R1, R2, and R3) and *Staphylococcus* (S1, S2, and S3) candidates were selected for further characterization by SDS-PAGE, and Western blotting. Western blotting was performed using sera from PN-allergic patients as well as sera from mice allergic to Ara h 1 or to Ara h 2, to identify IgE-binding epitopes in the digested PN allergens. Proteomic analysis using nano liquid chromatography coupled to mass spectroscopy was used to characterize the degradation products and PN-specific epitopes. For immune activation studies, bone marrow-derived mast cells (BMMCs) were cultured and sensitized to PN with sera from PN-allergic mice. These cells were challenged with bacterially digested PN to evaluate BMMC activation by β-hexosaminidase release and flow cytometry analysis of degranulation markers (CD63, CD107a).

METHOD DETAILS

Mouse colonization procedures

For colonization of GF C57BL/6 mice with ASF and SPF microbiota, fresh cecal and colon contents were harvested from SPF C57BL/6 mice (Taconic) or ASF C3H-HeN mice, diluted 1:10 in sterile PBS in anaerobic conditions, and 0.2 mL of each cecal/fecal suspension was orally gavaged to mice.

For mono-colonization of GF C57BL/6 mice with PN-degrading bacteria, *Rothia* R3 or *Staphylococcus* S1, S2, or S3 were grown o/n in brain heart infusion broth (BHI; Research products International Corp.) and 10^9 colony forming units (CFU) from the culture were provided by oral gavage with PBS as a vehicle. GF controls were provided PBS by oral gavage.

For PN anaphylaxis model, ASF C3H-HeNTac mice received 10^9 CFU total of *Rothia* R1, R2, and R3, by oral gavage, administered once per week for three weeks after sensitization and before PN challenge. Sterile PBS was used as a vehicle and served as

a non-colonization control. Colonization was confirmed one week after the final oral gavage by culturing mouse fecal suspensions on BHI agar plates. Bacteria were subsequently identified by PCR and Sanger sequencing as described below.

PN-specific IgE determination

Peripheral blood was collected by retro-orbital bleeding 48 h before the PN challenge. Serum PN-specific IgE was measured using a sandwich ELISA adapted from previously described methods[33]. Briefly, 96-well plates (high-binding, flat-bottom, polystyrene; Corning, USA) were coated o/n at 4°C with 2 µg/mL rat anti-mouse IgE antibody diluted in PBS. Plates were washed with PBS/0.05% Tween-20 (PBS-T; Sigma Aldrich), then blocked with 1% BSA in PBS-T for 2 h at room temperature (RT). Plates were washed thoroughly with PBS-T, then serum samples were incubated on the plate at 1/2 dilution o/n at 4°C. To detect PN-specific IgE, plates were incubated with biotinylated-CPE (biot-CPE; 0.1518 µg/mL in blocking solution) for 90 min at RT. Biot-CPE was generated using the EZ-Link Sulfo-NHS-LC-Biotinylation kit (Thermo Scientific). A standard curve, to which no capture antibody or sera was added, was generated using biot-CPE, serially diluted from 75 ng/mL to 0.6 ng/mL in PBS. Plates were washed thoroughly, then incubated with streptavidin-HRP (1:250 dilution in blocking solution; Thermo Scientific) and tetramethylbenzidine substrate (TMB; Thermo Scientific or Biolegend). The reaction was stopped with 1 N H_2SO_4. OD was measured at 450 nm, and the values were interpolated against the biot-CPE standard curve to determine relative PN-specific IgE binding. Results are expressed as PN-IgE (Relative Binding, OD), reflecting the ability of serum PN-specific IgE to bind PN allergens.

mMCP-1 quantification

Peripheral blood was collected by retro-orbital bleeding 40 min after the PN challenge. The concentration of mMCP-1 was quantified using a Mouse mMCPT-1 ELISA kit (Thermo Scientific) following the manufacturer's instructions. Briefly, serum samples were diluted by 1/25 and incubated on the capture antibody (anti-mouse mMCPT-1)-coated plate for 2 h at RT. After washing, a biotin-conjugated anti-mouse mMCPT-1 antibody was added to the plate and incubated for 1 h at RT. The reaction was developed with avidin-HRP and TMB, stopped with 1N H_2SO_4 and OD was measured at 450 nm. The results are expressed as ng of mMCP-1 per mL of serum and multiplied by the dilution factor of the sample.

ELISA detection of PN allergens in biological samples

Ara h 1 and Ara h 2 were detected in samples harvested 40 min following intra-gastric administration of 24 mg of CPE in 0.8 mL of PBS. Serum from peripheral blood was collected by retro-orbital bleeding and analyzed undiluted. Whole small and large intestinal content was analyzed after dilution by 1/5 and 1/10 in PBS. The quantification

of PN allergens was performed using proprietary ELISA kits for Ara h 1 and Ara h 2 following the manufacturer's instructions (Indoor Biotechnologies). Briefly, for Ara h 1 detection by ELISA (Indoor Biotechnologies): Plates pre-coated with a monoclonal anti-Ara h 1 antibody were washed with wash buffer, and biological samples and Ara h 1 standards were added and incubated for 1 h. The plates were washed, and a second monoclonal anti-Ara h 1 antibody conjugated to peroxidase was added and incubated for 1 h. After a final wash, TMB substrate was added, and the reaction was stopped with 0.5 N H_2SO_4. OD was measured at 450 nm, and results were expressed as the concentration of Ara h 1 in biological samples, multiplied by the dilution factor. For Ara h 2 detection by ELISA (Indoor Biotechnologies): Plates pre-coated with a monoclonal anti-Ara h 2 antibody were washed with wash buffer, and biological samples and Ara h 2 standards were added and incubated for 1 h. After washing, a rabbit anti-Ara h 2 polyclonal detection antibody was added and incubated for 1 h. This was followed by the addition of a peroxidase-conjugated anti-rabbit IgG for 1 h. After the final wash, TMB substrate was added, and the reaction was stopped with 0.5 N H_2SO_4. OD was measured at 450 nm, and results were expressed as the concentration of Ara h 2 in biological samples, multiplied by the dilution factor.

<u>Detection of PN degradation by microbes isolated from human saliva and mouse intestinal content</u>

Whole human saliva samples from healthy individuals (n=13) and mouse small and large intestinal contents (10 mg/mL in PBS) were plated on agar media plates designed to isolate PN-degrading bacteria. BHI media enriched with powdered PN (organic partially defatted PN; PB&Me, Sahah Naturals) or agar supplemented with powered PN were used. Plates were incubated with samples for 48 h in aerobic and anaerobic conditions (Bactron IV anaerobic chamber). The bacteria were isolated based on their capacity to generate a visible hydrolytic halo in the media, which is indicative of the breakdown of PN components in the media. Isolated bacteria demonstrating PN hydrolytic activity were incubated in liquid BHI with CPE (0.5 mg/mL). After 48 h of incubation under aerobic or anaerobic conditions, the amount of Ara h 1 and Ara h 2 in media was quantified by ELISA as described above and degradation capacity was displayed as a semi-quantitative measure by comparing the initial concentration of Ara h 1 and Ara h 2 in the non-growth negative control to the remaining concentration in the experimental samples.

Salivary and intestinal microbes were identified using Sanger sequencing technology. Briefly, DNA from isolates was extracted by picking single bacterial colonies into water, boiling, and centrifuging at 2,000 RCF for 2 min. The 8F-926R region of the 16S rRNA gene was amplified by PCR using the extracted DNA and sequences were determined using Sanger sequencing (FW primer: 5'- AGAGTTTGATCCTGGCTCAG-3', RV primer: 5'-CCGTCAATTCCT-TTRAGTTT-3'). The resulting sequences for the isolates were taxonomically assigned using the NCBI nucleotide collection database[86].

Microbial digestion of PN for challenge

Selected bacteria (*Rothia aeria* (R1), *Staphylococcus epidermidis* (S1), and *Staphylococcus aureus* (S3)) were grown o/n on BHI agar plates enriched with 1% powdered PN to confirm PN degradation capability (visible PN hydrolytic halo). For each strain, a 10 mL pre-inoculum was prepared by o/n culture in liquid BHI. Then, 10 µL of pre-inoculum was transferred into 5 mL of OptiMEM medium containing 30 mg/mL CPE and incubated for 6 h to complete the PN digestion process. The resulting digests were boiled for 5 min to kill the bacteria, and 800 µL of the digests, containing 24 mg of digested PN, was administered by oral gavage at the time of challenge as described above. OptiMEM medium served as the vehicle for non-digested CPE challenge.

Measurement of *ex vivo* intestinal PN-degrading capacity

The ability of the intestinal content from mice colonized with PN-degrading bacteria to degrade PN was assessed using ELISA and a bioassay with agar media enriched with PN. Solid BHI agar enriched with 1% powdered PN was prepared, and a 50 µL aliquot of diluted (1/2 in PBS) small intestinal content was placed into wells created in the agar. The plates were then incubated for 24 h. The PN-degrading capacity was determined by measuring the diameter of the clear halo around the inoculation site, indicating degradation, and the results were expressed in millimeters. In addition, the intestinal contents were also incubated with CPE (0.5 mg/mL). After 48 h of incubation, the quantity of Ara h 1 and Ara h 2 in media was analyzed by ELISA as described above.

Ussing chamber detection of PN translocation after bacterial digestion

Translocation of PN allergens after digestion by bacteria was evaluated *ex vivo* using small intestinal sections of SPF C3H-HeN mice and the Ussing chamber technique. For preparation of bacterial PN allergen digestions, *Rothia mucilaginosa* (R3), *Staphylococcus epidermidis* (S1), and *Staphylococcus aureus* (S2 & S3) were grown for 16 h in BHI liquid medium. Bacteria were then incubated in BHI with 5 mg/mL CPE for 4 h to allow for bacterial digestion of the PN allergens. After incubation, samples were boiled for 15 min. Bacterial digestions were performed in triplicate, with a negative control containing no bacterial inoculum. For the Ussing chamber technique, 1.5 cm sections of proximal small intestine were collected, opened along the mesenteric border, and mounted on the sliders of Ussing chambers. Each chamber exposed 0.25 cm^2 of tissue surface area to 4 mL of circulating oxygenated Krebs buffer containing 10 mM glucose (serosal side) and 10 mM mannitol (mucosal side), maintained at 37°C and aerated with 95% O_2 and 5% CO_2. Then, 0.2 mL of each bacterial digestion was placed into 4 mL of Krebs buffer on the mucosal side of the chamber. The experiment was run for 2 h, after which the total mucosal and serosal volumes were collected. The concentrations of PN allergens Ara h 1 and Ara h 2 on the serosal side were quantified by ELISA and expressed as intestinal translocation of allergens. The Ussing chamber system was from Physiologic Instruments.

Microbial digestion of PN for proteomic and immune activation assays

Rothia (R1- *Rothia aeria* R2- *Rothia dentacariosa* R3- *Rothia mucilaginosa*) and *Staphylococcus* (S1- *Staphylococcus epidermidis,* S2- *Staphylococcus aureus,* S3- *Staphylococcus aureus*) species were selected for characterization of PN allergen degradation and allergenicity. Bacteria were grown o/n in BHI (10 mL), then 10 µL of bacterial culture was taken and used to inoculate 1 mL of OptiMem with 0.5 mg/mL CPE. The bacteria were incubated in the media with CPE for 4 h at 37ºC. After the incubation, the digestion was stopped by boiling for 5 min. Subsequently, the digestion of Ara h 1 and Ara h 2 were detected using ELISA, SDS-PAGE and Western blotting, and BMMC activation assays.

SDS-PAGE and Western blotting

To assess PN degradation profiles produced by degradation by *Rothia* and *Staphylococcus* species we performed SDS-PAGE and Western blotting. Bacteria were grown in 0.5 mg/mL as mentioned above. Undigested PN, was used as control. Then Laemmli sample buffer (Bio-Rad) with β-mercaptoethanol (Sigma-Aldrich) at 1/10 was added at 1/4 in a final volume of 50 µL. Before loading the gel (Any kD™ Mini-PROTEAN® TGX™ Precast Protein Gels, Bio Rad), samples were heat-denatured at 100ºC for 5 min. Moreover, a protein molecular weight marker was added (ThermoFischer). The gel was run in 1X running buffer (*i.e.*, SDS/Tris/Glycine 10X, Bio-Rad) for 1-1.5 h at 100 V using an electrophoretic cell and a power supply Mini-Protean System Bio-Rad (Bio-Rad).

For SDS-PAGE, after running, the gel was placed in staining solution (45% of methanol and 10% of acetic acid in distilled water, plus 0.2% w/v of Coomassie blue, Bioscience) for 1 h in agitation. Then, the staining solution was removed using destaining solution (20% methanol and 10% acetic acid, Sigma-Aldrich, in distilled water) in constant agitation, the process was repeated every 15 min until the background was eliminated. Then, the gel was photographed using a molecular imaging system (Amersham ImageQuant™ 800).

For Western blotting, after running the gel, the bands of the gel were transferred to a nitrocellulose membrane (Bio-Rad) using a transfer system (fiber pad, filter paper, membrane, gel, filter paper and fiber pad) and transfer buffer (20% methanol and 10% of Tris-Glycine 1X in distilled water). The transference was run for 1 h at 400 mA. Then, to check that bands were transferred correctly, the membrane was stained with Ponceau S Staining solution (ThermoScientific). After cleaning with water and 3 washes with TBS-T solution, the membrane was blocked in constant agitation for at least 1 h with 3% BSA (NZYtech) in TBS-T. Then, the membrane was incubated with sera from PN-allergic donors, or sera from mice allergic to Ara h 1 or to Ara h 2 (diluted in 3% BSA at different dilutions depending on the amount of IgE) as primary antibody, at 4ºC o/n with smooth agitation. Sera from non PN-allergic donors **(Table S2)** and non PN-allergic mice were

used as negative control. During day 2, after performing 6 washes with TBS-T every 10 min with agitation, the membrane was incubated with anti-human IgE-HRP (Invitrogen) 1:10,000 or anti-mouse IgE-HRP (SouthernBiotech) 1:1,000 as secondary antibody for 1 h at RT with agitation. Then, 6 washes with TBS-T every 10 min with agitation were performed before revealing the membrane According to the instructions of the manufacturer (Cytiva-Merck), 1:1 of peroxide and luminol and 1 mL of the mixture was added to the membrane. The chemiluminescent signal of the gel was captured in a chemiluminescent imaging system (Amersham ImageQuant™ 800). SDS-PAGE and Western blots were analyzed using Fiji ImageJ.

Proteomics

Proteomics was performed to identify bacterial degradation products of PN allergens and to map PN-specific epitopes. Microbial PN digestions (above) by *Rothia* (R1, R2, and R3) and *Staphyloccocus* (S1, S2, and S3) were ultra-filtered using microcon filter units with a 3 kD cutoff that were previously equilibrated and washed with water. The peptides of the flow-through were selected (<3 kD) and they were cleaned with ZipTip with 0.6 µL C18 resin (Merck Millipore) to avoid the presence of elements that could interfere with the mass spectrometry, and they were drained in a SpeedVac Vacuum Concentrator. The samples, resuspended in a volume of 14 µL and 2 µL LC-MS grade water containing 2% (v/v) acetonitrile and 0.1% (v/v) formic acid, were used for the quantification with the QBIT method, analyzing around 0.8 µg per sample. The peptides were analyzed by nano liquid chromatography coupled to mass spectrometry in data-dependent-acquisition mode using an UltiMate 3000 High Pressure Liquid Chromatograph (Fisher Scientific) and a Orbitrap Exploris™ 240 Mass Spectrometer (Fisher Scientific). The flow of the chromatograph was 250 nL/min for 60 min, and an Easy-spray PepMap C18 analytical column 50 cm × 75 µm (Fisher Scientific) was used.

The obtained MS1 and MS2 spectra were analyzed using the Peaks (https://www.bioinfor.com/peaksdb/) search engine against an *Arachis hypogaea* proteome database obtained from UniprotKB (https://www.uniprot.org/) combined with a list of typical laboratory contaminants, using a tolerance of 10 ppm and 0.02 Da for the precursor ions and fragments, respectively. Carbamidomethylation in cysteines was used as fixed modification and acetyl in the N-terminal end of the protein and methionine oxidation were used as variable modifications. The search was performed without restrictions to any proteases and the results were shown as proteins identified with at least a unique peptide with a False Discovery Rate ≤1%.

The unique peptides obtained after the analysis were located and identified in the sequences of Ara h 1 and Ara h 2, which were downloaded from the Protein Data Bank (https://www.rcsb.org/). The most common human IgE binding epitopes of Ara h 1 and Ara h 2 were found in the following allergen databases: Allergen Nomenclature

(https://allergen.org/); Allergen Online (http://allergenonline.org/); and Compare Database (https://db.comparedatabase.org/). Furthermore, previous studies were considered to specify immunodominant IgE binding epitopes[29-31]. Molecular structure analysis was performed with Chimera v1.17.3 for tridimensional visualization of allergens and relevant epitopes before and after bacterial digestion.

Mice sensitization to Ara h 1 and Ara h 2

Mice were sensitized to immunodominant PN allergens to generate sera specific to Ara h 1 or Ara h 2 specific IgE to be used in mast cell degranulation assays (above). To sensitize mice against native Ara h 1 (InBio) or recombinant Ara h 2 (prepared as reported[87] using Uniprot reference Q6PSU2-1 without the signal peptide), 3 intraperitoneal injections with 10 µg of the allergen plus 1 mg aluminum hydroxide (Alhydrogel® adjuvant 2%, InvivoGen) were performed. Previously, aluminum hydroxide and allergen were mixed at 4ºC during 30 min in a ferris wheel. Between the first and second injection, 2 weeks were left; and 1 week between the second and third injection. Blood samples were collected and centrifuged at 16,000 RCF to obtain sera for mast cell activation assays and Western blot analysis (see below). Control sera from PN-allergic mice were generated following immunization with a classical model of food allergy.[33,52]

Bone marrow-derived mast cell culture

BMMCs were cultured to assess mast cell activation by bacterially digested PN allergens. Bone marrow from femur and tibia of C57BL/6 (Charles River) mice were used to obtain BMMCs as described[88]. In short, bone marrow was flushed out inserting a 23-gauge needle (BD Microlance) attached to the 10 mL syringe filled with PBS (Gibco) at the knee side of both types of bone. Then, the cell suspension collected was filtered with a 40 µm filter (Falcon). After centrifugating 5 min at 286 RCF and RT, the pellet was lysed with ACK lysing buffer (Lonza). Erythrocyte-lysed bone marrow cells were cultured for 4 weeks in Petri dishes at 37ºC and 5% CO_2 in Iscoves´s Modified Dulbecco´s Medium (IMDM, Gibco) supplemented with 10% fetal bovine serum (FBS, Cytiva), 1% minimal essential medium (MEM, Gibco), 1% sodium pyruvate (Biowest), 1% penicillin/streptomycin (P/S, Gibco), 1% non-essential amino acids (Biowest), 0.01% recombinant murine stem cell factor (SCF, PeproTech) and 0.05% recombinant murine Interleukin (IL-3, PeproTech), until they differentiated into mature BMMCs. Cell growth and viability were monitored using the trypan blue exclusion test. The culture media was changed weekly, and the cellularity was kept below 0.5×10^6 cells/mL.

BMMC activation

BMMC activation was conducted as reported[32,33]. In brief, BMMCs were sensitized o/n at 37ºC and 5% CO_2 with sera at a concentration range of 15–40 ng/mL from Ara h 1- or Ara h 2-sensitized mice. Culture media was changed 1-2 days previous sensitization. PN-allergic mice sera were used as a positive control. BMMC sensitization was done at a cell

density of 1 × 10^6 cells/mL. The next day, BMMCs were washed to eliminate unbound Igs (cells were spun at 265 RCF for 5 min and low break) and resuspended in supplemented IMDM without cytokines, nor FBS, at a cell density of 1 × 10^6 cells/mL. For BMMC activation, bacteria with PN-degrading potential isolated from saliva and gut of healthy donors were selected. Then, 0.1 × 10^6 BMMCs per condition were placed in a U/V bottom 96-well culture plate (Falcon) and challenged with bacterially digested PN (Stallergenes Greer) at 25 µg/mL and 100 µg/mL in Ara h 1-sensitized BMMCs, or at 50 µg/mL and 200 µg/mL in Ara h 2-sensitized BMMCs. Media and undigested PN were used as negative and positive controls, respectively. After 20 min at 37ºC and 5% CO_2, the reaction was stopped on ice and BMMC activation was determined via β-hexosaminidase activity in the supernatants, and phenotypically (CD63 and CD107a expression) by flow cytometry[32].

β-hexosaminidase activity assay

BMMCs were centrifugated as above described to recover cell-free supernatants. A volume of supernatant of 45 µL was added in duplicates to 45 µL of β-hexosaminidase substrate solution (2 mM p nitrophenyl N-acetyl β-D-glucosamine, Sigma-Aldrich) diluted in 0.1 M citrate buffer (45 mM dehydrated sodium citrate, 55 Mm citric acid, Sigma-Aldrich, in distilled H_2O) in a flat-bottom 96-well plate. After incubation at 37ºC for 45 min in the dark, 45 µL NaOH 1 M (1M sodium hydroxide, Sigma-Aldrich, in distilled H_2O) were added to stop the reaction. OD was measured at 405 nm with a microplate reader. Buffers alone and BMMC lysates (0.5% Triton X-100, Sigma Aldrich, was used for cell lysis) were used as control, absorbance background (B) and total lysis, respectively. The percentage of BMMC degranulation, based on β-hexosaminidase activity, was calculated as follows:

$$\text{Degranulation (\%)} = \frac{\text{OD supernatant-B}}{\text{OD total lysis-B}} \times 100$$

Flow cytometry

BMMCs were resuspended in ice-cold FACS buffer (2.5 mM EDTA, PanReacAppliChem, 0.5% BSA in PBS). BMMCs were blocked with 1:50 Fc block (purified anti-mouse CD16/32, BioLegend) for 15 min on ice to prevent non-specific antibody binding. Then, BMMCs were incubated with BV421 rat anti-CD117 (c-kit) (BioLegend) 1/200; APC rat anti-CD63 (BioLegend) 1:200; PerCP-Cy5.5 rat anti-CD107a (LAMP-1) (BioLegend) 1:200; PE rat anti-IgE (BioLegend) 1:200; PE-Cy7 rat anti-FcεR1α (BioLegend) 1:200; on ice for 30 min covered from light. Viability was assessed with efluor780 dye (eBioscience) 1:4,000. After washing with FACS buffer to eliminate unbound antibodies, cells were analyzed on a BD FACSCantoll flow cytometer. On average, 10,000 events of live and singlet cells were recorded. Data were analyzed with FlowJo v10 software; dead cells and aggregates were excluded and fluorescence minus one (FMO) controls were used for gating.

Microbiota analysis

DNA was extracted from mouse fecal pellets and human saliva and the hypervariable V3-V4 regions of the 16S rRNA gene were amplified with polymerase chain reaction (PCR) using Taq polymerase (Life Technologies), as previously described[63]. Forward barcoded primers targeting the V3 region (v3f_341f-CCTACGGGNGGCWGCAG) and reverse primers targeting the V4 region (v4r_806r-GGACTACNVGGGTWTCTAAT) were used. Forward primers included six-base pair barcodes to allow multiplexing samples. Purified PCR products were sequenced using the Illumina MiSeq platform by the McMaster Genomics facility. Primers were trimmed from the obtained sequences with Cutadapt software[89,90], and processed with Divisive Amplicon Denoising Algorithm 2 (DADA2; version 1.14.0) using the trained SILVA reference database (version 138.1)[91,92]. A phylogenetic tree of the sequences was calculated using FastTree 2[93], and data was explored using the phyloseq package (version 1.30.0) in R (version 3.6.2)[94]. After data cleanup, a total of 292,618 reads were obtained with a minimum of 11,651 and maximum of 60,790 with an average of 32,513 reads per sample for mouse microbiota. For human healthy control salivary microbiota, a total of 273,686 reads were obtained with a minimum of 1,881 and maximum of 48,620 with an average of 16,099 reads per sample. For PN allergic patient salivary microbiota, a total of 844,167 reads were obtained with a minimum of 3,236 and maximum of 145,324 with an average of 36,702 reads per sample. Alpha-diversity was measured using observed species and Chao1 indices. Beta-diversity was calculated on normalized data and the originated matrices were ordinated using principal coordinate analysis based on Jaccard distance (mouse microbiota) and Bray-Curtis dissimilarity (human microbiota).

STATISTICAL ANALYSIS

All variables were analyzed using GraphPad Prism 9 and 10 software (GraphPad Software, USA). Parametric data are depicted as dot plots with each dot representing an individual mouse or biological replicate. Normal distribution was determined by D'Agostino-Pearson omnibus normality test, Shapiro-Wilk test, and Kolmogorov-Smirnov test with Dallal-Wilkinson-Lillie correction. One way analysis of variance (ANOVA) was used to evaluate differences between more than two groups with a parametric distribution and Tukey's or Dunnet's post-hoc corrections were applied. Student's t-test (two-tailed) was performed to evaluate the differences between two independent groups as appropriate. Data with non-normal distribution were evaluated with Kruskal-Wallis test with Dunn's post-hoc test for more than two groups. A P value of ≤ 0.05 was selected to reject the null hypothesis. Information regarding specific P values, value of n, and how data are presented can be found in figure legends.

KEY RESOURCES TABLE

REAGENT or RESOURCE	SOURCE	IDENTIFIER
Antibodies		
Rat anti-mouse IgE (clone R35-72)	BD Pharmingen	Cat# 553413
Anti-mouse IgE-HRP (clone: 23G3)	SouthernBiotech	Cat#1130-05
Anti-human IgE-HRP	Invitrogen	Cat#A18793
Sera from Ara h 1- or Ara h 2-sensitized mice	This paper	N/A
Purified anti-mouse CD16/32 (clone: 93)	BioLegend	Cat#101302
BV421 rat anti-CD117 (c-kit) (clone: ACK2)	BioLegend	Cat#135124
APC rat anti-CD63 (clone: NVG-2)	BioLegend	Cat#143906
PerCP-Cy5.5 rat anti-CD107a (LAMP-1) (clone: 1D4B)	BioLegend	Cat#121626
PE rat anti-IgE (clone: RME-1)	BioLegend	Cat#406908
PE-Cy7 rat anti-FcεR1α (clone: MAR 1)	BioLegend	Cat#134318
Bacterial and virus strains		
Rothia aeria	This paper	R1
Rothia dentacariosa	This paper	R2
Rothia mucilagenosa	This paper	R3
Staphylococcus epidermidis	This paper	S1
Staphylococcus aureus	This paper	S2
Staphylococcus aureus	This paper	S3
Biological samples		
Serum from peanut-allergic donors	Hospital Universitario de la Princesa	N/A
Saliva from Healthy controls	McMaster University	N/A
Saliva from peanut-allergic patients	Mass General Hospital	N/A
Chemicals, peptides, and recombinant proteins		
ACK Lysing Buffer	Lonza	Cat#BP10-548E
Iscoves´s Modified Dulbecco´s Medium (IMDM)	Gibco	Cat#12440-053
Fetal Bovine Serum (FBS)	Cytiva	Cat#SV30160.03
Minimal essential medium (MEM)	Gibco	Cat#11120-037
Penicillin/Streptomycin	Gibco	Cat#15140122
Non-essential amino acids	Biowest	Cat#X0557-100
Sodium Pyruvate	Biowest	Cat#L0642
Recombinant Murine Stem Cell Factor (r-mSCF)	PeproTech	Cat#250-03
Recombinant Murine Interleukin 3 (r-mIL-3)	PeproTech	Cat#213-13
Native Ara h 1	InBio	Cat#NA-AH1-1
Native Ara h 2	InBio	Cat#NA-AH2-1
Recombinant Ara h 2	Centre for Plant Biotechnology and Genomics	N/A
Aluminum hydroxide, Alhydrogel® adjuvant 2%	InvivoGen	Cat#21645-51-2
Bovine Serum Albumin (BSA)	NZYtech	Cat#9048-46-8
Tetramethylbenzidine (TMB)	Biolegend	Cat#421101
Peanut (PN; CPE)	Stallergenes Greer	Cat#XPF171D3A25
p nitrophenyl N-acetyl β-D-glucosamine	Sigma-Aldrich	Cat#N9376-100MG
0.5% Triton X-100	Sigma Aldrich	Cat#9036-19-5
Ethylenediaminetetracetic acid (EDTA)	PanReacAppliChem	Cat#131026
Efluor780 viability	eBioscience	Cat#65-0865-14

Any kD™ Mini-PROTEAN® TGX™ Precast Protein Gels	Bio Rad	Cat#4569034
Nitrocelulose membrane	Bio Rad	Cat#1620115
Protein molecular weight marker	ThermoFischer	Cat#26619
Microcon units	Sigma	Cat#UFC5003
Cholera toxin from *Vibrio cholerae* Inaba 5698	List Biological Laboratories	Cat#100B, 9100B
Brain-heart infusion (BHI) broth	Research Products International Corp.	Cat#B11000-1000
Powdered PN	PB & Me, Sahah Naturals	SKU#62845116652
Opti-MEM™ Reduced Serum Medium	Gibco, ThermoScientific	Cat#31985070
Critical commercial assays		
Mouse MCpT-1 Uncoated ELISA Kit with Plates	Thermo Scientific	Cat#88-7503-22
Ara h 1 ELISA 2.0	Indoor Biotechnologies	Cat#EPD-AH1-5
Ara h 2 ELISA 2.0	Indoor Biotechnologies	Cat#EPD-AH2-5
EZ-Link Sulfo-NHS-LC-Biotinylation Kit	ThermoScientific	Cat#21435
Deposited data		
Microbiome data (TBD)		
Experimental models: Cell lines		
Experimental models: Organisms/strains		
Mouse:C57BL/6 (6–12 weeks of age, male or female)	Charles River Laboratory	Strain No.: 027
Mouse:C3H-HeN	Taconic Biosciences	Strain No.: C3H/HeNTac
Mouse:C57BL/6N (germ-free)	Taconic Biosciences	Strain No.: C57BL/6NTac
Oligonucleotides		
Microbiota primers F: (v3f_341f-CCTACGGGNGGCWGCAG) R: (v4r_806r-GGACTACNVGGGTWTCTAAT)	IDT DNA	N/A
Sanger sequencing primers F: (5'- AGAGTTTGATCCTGGCTCAG-3') R: (5'-CCGTCAATTCCT-TTRAGTTT-3')	IDT DNA	N/A
Recombinant DNA		
Software and algorithms		
Graph Pad Prism v 9.0	GraphPad	https://www.graphpad.com/demos/
FlowJo v10	BD	https://www.flowjo.com/solutions/flowjo
Peaks	Bioinformatics Solutions Inc.	https://www.bioinfor.com/peaksdb/
UniprotKB	Uniprot	https://www.uniprot.org/
Protein Data Bank	RCSB PDB	https://www.rcsb.org/

Allergen Nomenclature	Allergen Nomenclature. Financial contributions from IUIS, EAACI, and AAAAI	https://allergen.org/
Allergen Online	AllergenOnline. University of Nebraska-Lincoln	http://allergenonline.org/
Compare Database	Compare	https://db.comparedatabase.org/
Chimera v1.17.3	University of California San Francisco (UCSF)	https://www.cgl.ucsf.edu/chimera/
ImageJ 1.53q	Fiji	https://fiji.sc/
Illumina MiSeq	Illumina Inc.	https://www.illumina.com/
Cutadapt	Marcel Martin[1]	https://cutadapt.readthedocs.io/
DADA2 (version 1.14.0)	Benjamin Callahan[2]	https://benjjneb.github.io/dada2/
SILVA Database (version 138.1)	SILVA Consortium[3]	https://www.arb-silva.de/
FastTree 2	Morgan N. Price et al.[4]	https://www.microbesonline.org/fasttree/
Phyloseq (version1.30.0)	Paul J. McMurdie & Susan Holmes[5]	https://joey711.github.io/phyloseq/
R (version 3.6.2)	R Foundation for Statistical Computing	https://www.r-project.org/
Other		
Sterile Dish 100 mm x 20 mm CC-treated	Corning	Cat#430167
U/V-bottom 96 well TC-treated microplates	Falcon	Cat#353910
Flat-bottom 96 well high binding microplates	Costar	Cat#3590
23-gauge needle	BD Microlance	Cat#300800
40 µm filter	Falcon	Cat#352340
Microplate reader	Promega	GloMax Discover
SalivaBio Children's Swab	Salimetrics	Cat#5001.06
Flow cytometer	BD	FACSCantoII
Ussing chamber system	Physiologic Instruments	Cat#P2400
Imaging system	Amersham	ImageQuant™ 800
ZipTip with 0.6 µL C_{18} resin	Merck Millipore	Cat#ZTC18S008
UltiMate 3000 High Pressure Liquid Chromatograph	Fisher Scientific	Cat# IQLAAAGABHFAPBMBFB
Orbitrap Exploris™ 240 Mass Spectrometer	Fisher Scientific	Cat#BRE725535
Easy-spray PepMap C18 analytical column 50 cm × 75 µm	Fisher Scientific	Cat#ES903
Non-heparinizing microcapillaries (Fisher Scientific),	Fisher Scientific	Cat#11884040

References

1. Martin, M. (2011). Cutadapt removes adapter sequences from high-througput sequencing reads. EMBnet.journal *17*, 10-12. https://doi.org/10.14806/ej.17.1.200.
2. Callahan, B.J., McMurdie, P.J., Rosen, M.J., Han, A.W., Johnson, A.J., and Holmes, S.P. (2016). DADA2: High-resolution sample inference from Illumina amplicon data. Nat Methods *13*, 581-583. 10.1038/nmeth.3869.
3. Quast, C., Pruesse, E., Yilmaz, P., Gerken, J., Schweer, T., Yarza, P., Peplies, J., and Glockner, F.O. (2013). The SILVA ribosomal RNA gene database project: improved data processing and web-based tools. Nucleic Acids Res *41*, D590-596. 10.1093/nar/gks1219.
4. Price, M.N., Dehal, P.S., and Arkin, A.P. (2010). FastTree 2--approximately maximum-likelihood trees for large alignments. PLoS One *5*, e9490. 10.1371/journal.pone.0009490.
5. McMurdie, P.J., and Holmes, S. (2013). phyloseq: an R package for reproducible interactive analysis and graphics of microbiome census data. PLoS One *8*, e61217. 10.1371/journal.pone.0061217.

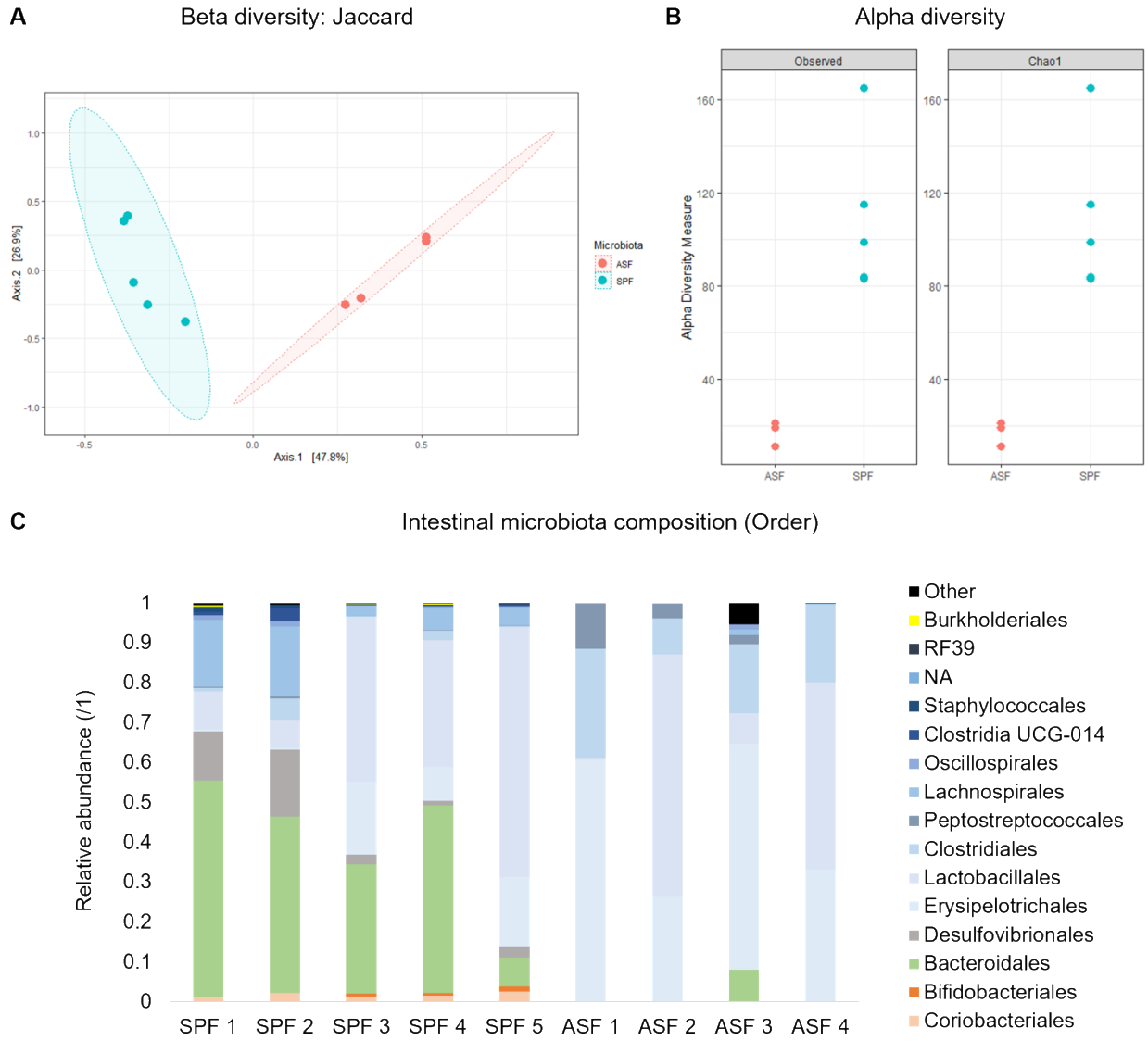

Figure S1. Intestinal microbiota of Altered Schaedler Flora (ASF) and specific pathogen free (SPF) mice. (A) Beta-diversity (Jaccard index) plot of fecal microbiota of ASF and SPF mice where each dot represents one mouse. (B) Alpha diversity metrics based on observed species and Chao1 index of ASF and SPF mice where each dot represents one mouse. (C) Order-level relative abundance of the microbial composition of ASF and SPF mice where each bar represents one mouse. n=4–5 mice per group.

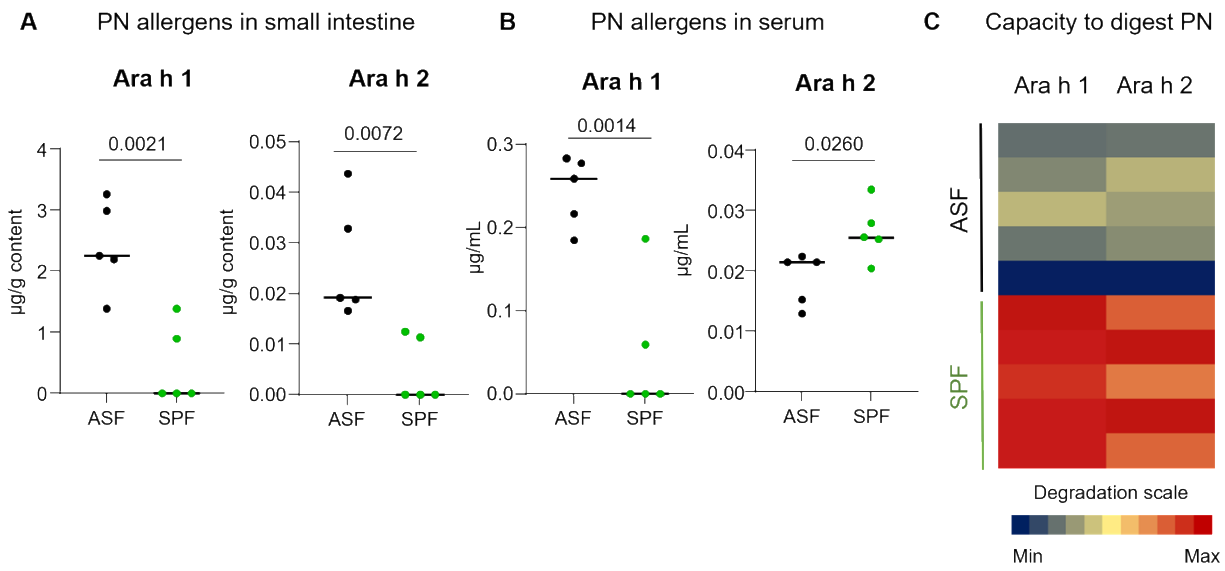

Figure S2. Peanut (PN) digestion by Altered Schaedler Flora (ASF) and specific pathogen-free (SPF) intestinal contents of C3H-HeN mice. ASF and SPF C3H-HeN mice were provided a 24 mg bolus of PN i.g. Peripheral blood and small intestinal contents were collected 40 minutes post PN delivery for analysis. n=5 mice per group. PN allergens (Ara h 1 and 2) in small intestinal content (A) and in serum from peripheral blood (B). (C) Heatmap showing digestion capacity of ASF and SPF microbiota of C3H-HeN mice against Ara h 1 and 2. Intestinal contents were subsequently incubated with PN allergens *in vitro* and remaining allergens were quantified after digestion. Each row represents one mouse. Significance levels: Ara h 1 SPF vs. ASF (P<0.0001), Ara h 2 SPF vs. ASF (P= 0.0001). Data are presented as mean where each dot represents an individual mouse (A-B), or each row represents one mouse (C). Displayed P values were calculated using an unpaired Student's *t*-test.

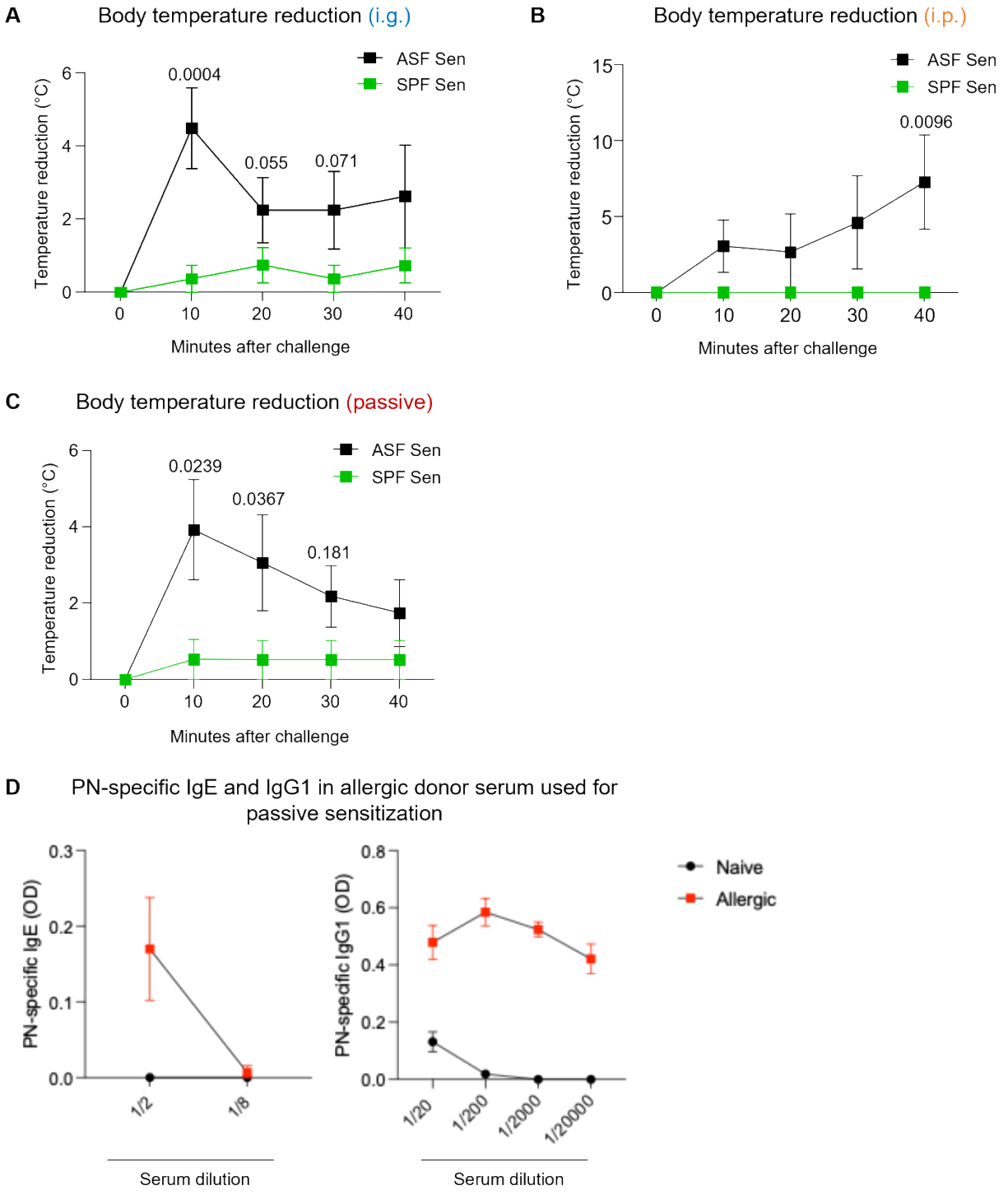

Figure S3. Body temperature reduction of Altered Schaedler Flora (ASF) and specific pathogen-free (SPF) mice in response to peanut (PN) challenge in different sensitization models, and characterization of allergic donor serum used for passive sensitization corresponding to Figure 2. (A-C) Body temperature reduction after PN challenge for i.g., i.p., and passively sensitized mice, respectively. (D) PN-specific IgE and IgG1 in allergic donor serum used for passive sensitization. Data are presented as mean + SD. Displayed *P* values were calculated using an unpaired Student's *t*-test.

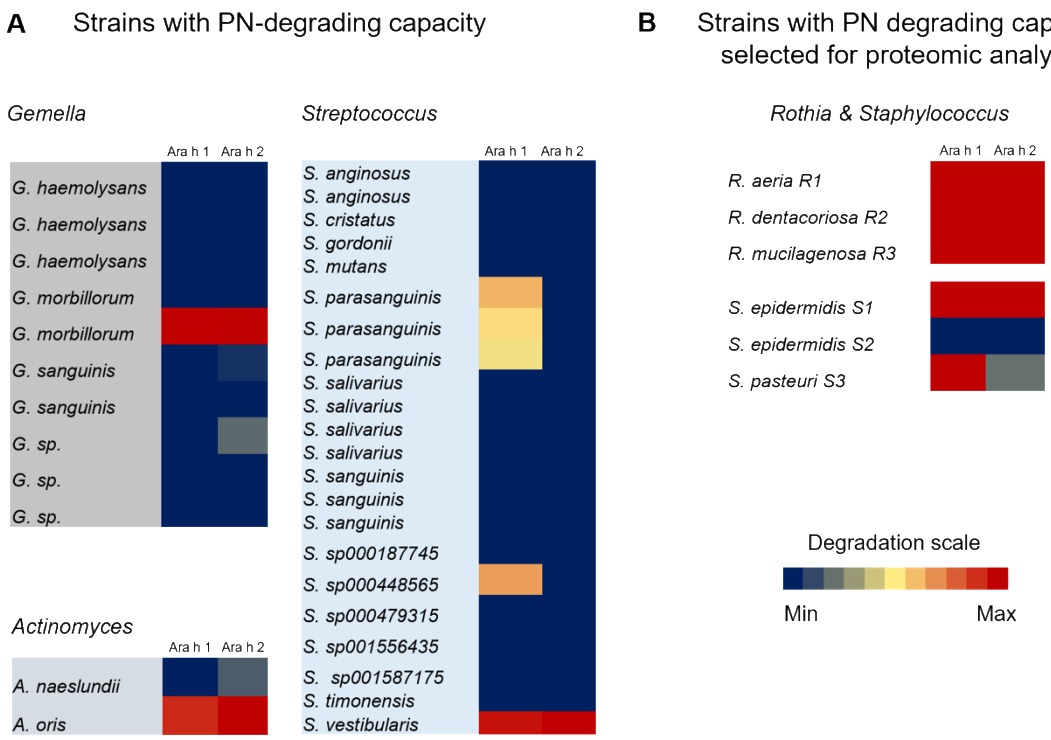

Figure S4. Characterization of peanut (PN)-degrading bacteria isolated from human saliva. (A) Heatmap of PN allergen degradation capacity of bacterial strains. (B) Degradation of Ara h 1 and 2 by bacterial strains that were further characterized in Figures 4 and 5 for their proteomic profiles and effects on mast cell activation. Colour scale (blue-yellow-red) represents allergen degradation.

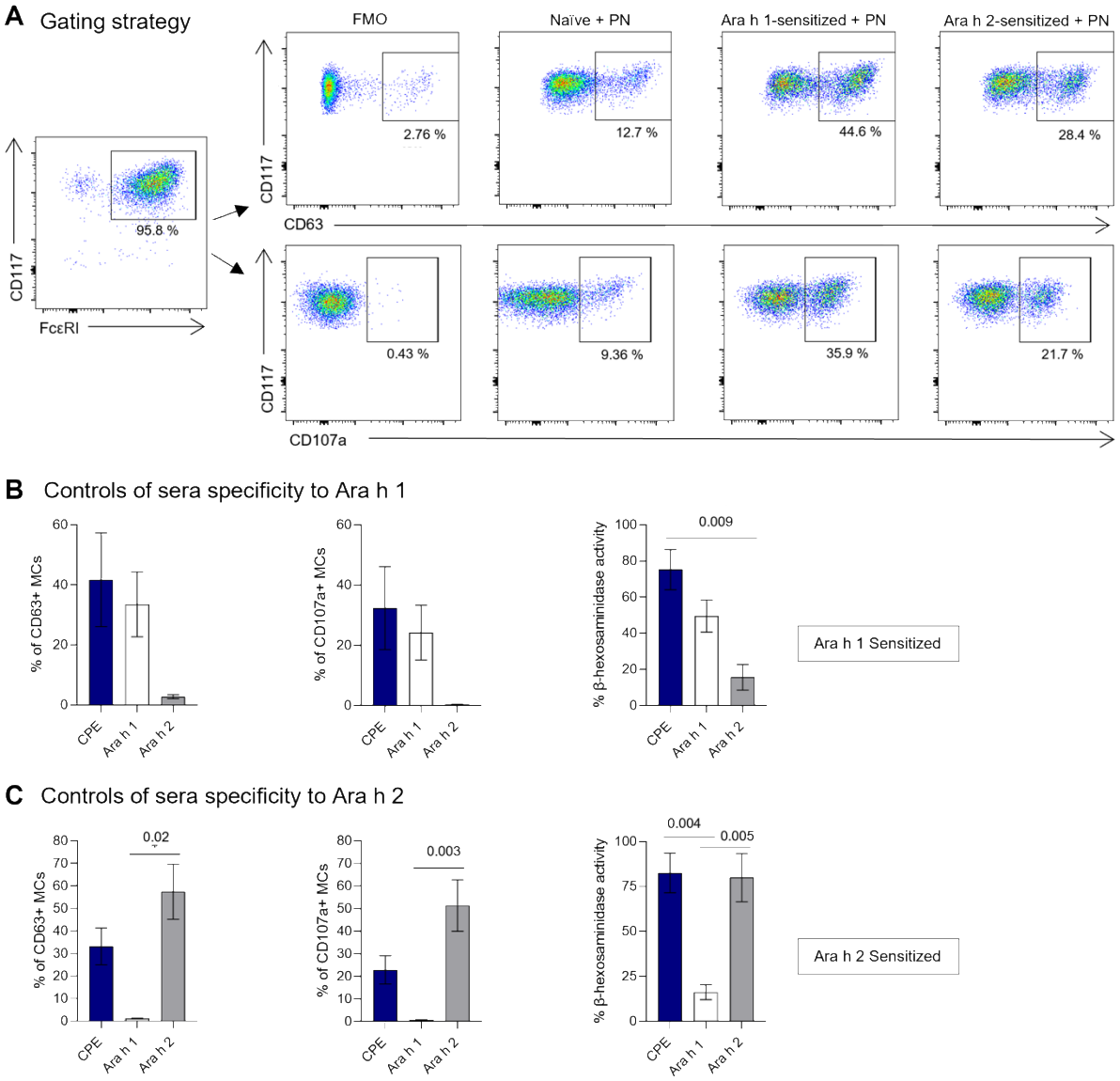

Figure S5. Characterization of sera specificity from mono-sensitized mice. (A) Gating strategy. Bone marrow-derived mast cells (MCs) co-express FcεRI and CD117. MC activation was detected by the expression of CD63 and CD107a. Gates of positive and negative controls are shown. Controls of sera specificity to (B) Ara h 1 and (C) Ara h 2. MCs were sensitized with a pool of sera from Ara h 1- or Ara h 2-allergic mice, respectively, and then challenged with undigested PN (blue), native Ara h 1 (white) or recombinant Ara h 2 (grey). Data are presented as the mean +/- SEM of each group. Displayed *P* values were calculated using a one-way ANOVA with Tukey's post-hoc test in panels B and C (CD107a and β-hexosaminidase activity) or using Kruskal-Wallis test with Dunn´s post hoc test in panel C (CD63).

A

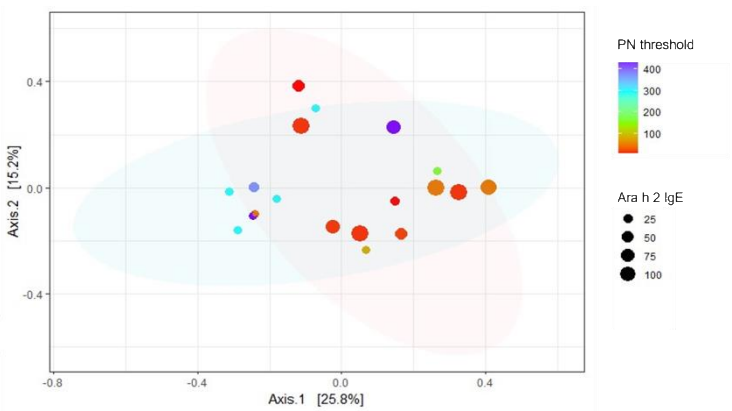

Figure S6. Peanut (PN)-allergic patients (n=19) were tested for PN threshold using increasing PN concentrations before enrolment in oral immunotherapy (OIT). (A) Bray-Curtis-based principal coordinate analysis of the microbiota of PN-allergic patients. Dot size represents serum Ara h 2-specific IgE levels, while dot colour corresponds to the PN threshold (scales shown).

Table S1: Detailed subject demographics. Peanut, PN; Male, M; Female; F.

Status	ID	Sex	Age	Race	PN threshold (mg)	Ara h 1 IgE (kUA/mL)	Ara h 2 IgE (kUA/mL)
PN-allergic	PN1	F	10	Unknown	300	0.10	1.19
	PN2	F	7	Asian	300	0.10	2.44
	PN3	F	1	White	300	0.10	0.10
	PN4	F	27	White	440	15.2	13.8
	PN5	F	6	White	375	20.3	25.7
	PN6	M	6	White	40	11.6	0.41
	PN7	M	7	White	300	N/A	N/A
	PN8	F	15	White	440	17.3	12.1
	PN9	M	9	White	12	100	25.8
	PN10	M	13	White	6	9.11	0.19
	PN11	M	10	White	43	18	88.5
	PN12	F	13	White	13	100	58.2
	PN13	F	13	White	43	100	100
	PN14	F	14	White	12	100	96.7
	PN15	M	9	White	6	5.95	20.7
	PN16	M	11	Asian	160	7.62	9.92
	PN17	F	2	Asian	80	1.41	0.84
	PN18	F	2	Black/African American	15.5	0.18	40.1
	PN19	M	4	Unknown	12	16.7	100
Non-PN-allergic	HV1	M	35	White	N/A	N/A	N/A
	HV2	M	22	White			
	HV3	M	20	White			
	HV4	F	26	White			
	HV5	F	33	White			
	HV6	F	24	White			
	HV7	F	18	White			
	HV8	M	30	White			
	HV9	F	38	White			
	HV10	F	20	Black/African American			
	HV11	M	40	Asian			
	HV12	F	66	White			
	HV13	M	33	White			

Table S2: Serum characterization for western blotting. Peanut, PN.

Serum	Total IgE levels (kU/L)	PN IgE (kUA/mL)	rAra h 1 IgE (kUA/mL)	rAra h 2 IgE (kUA/mL)	rAra h 3 IgE (kUA/mL)	rAra h 8 IgE (kUA/mL)	rAra h 9 IgE (kUA/mL)	Sex	Age	Positive Skin Prick Test	Other hypersensitivities
A	12,49	Unknown	52.9	>100	26.6	0.02	0.02	F	30	PN, pollen of Cupressaceae, Acer pseudoplatanus, olive, grasses, Salsola, dog, cat, horse and rabbit. Minimal reaction to mites and aspergillus	Persistent moderate asthma and intermittent rhinoconjunctivitis
B	176	54.9	20.4	24.5	0	0	0	F	19	PN, chickpea, arizonica pollen, minimal reaction to pine nuts	Atopic dermatitis